


December 2017

Clinical Near-infrared Spectroscopy Instrumentation: Postural Orthostatic Tachycardia Syndrome Studies

Parvathi Kadamati

University of Wisconsin-Milwaukee

Follow this and additional works at: <https://dc.uwm.edu/etd>

 Part of the [Biomedical Engineering and Bioengineering Commons](#), and the [Electrical and Electronics Commons](#)

Recommended Citation

Kadamati, Parvathi, "Clinical Near-infrared Spectroscopy Instrumentation: Postural Orthostatic Tachycardia Syndrome Studies" (2017). *Theses and Dissertations*. 1648.
<https://dc.uwm.edu/etd/1648>

This Thesis is brought to you for free and open access by UWM Digital Commons. It has been accepted for inclusion in Theses and Dissertations by an authorized administrator of UWM Digital Commons. For more information, please contact open-access@uwm.edu.

CLINICAL NEAR-INFRARED SPECTROSCOPY
INSTRUMENTATION: POSTURAL ORTHOSTATIC
TACHYCARDIA SYNDROME STUDIES

by

Parvathi Kadamati

A Thesis Submitted in

Partial Fulfillment of the

Requirements for the Degree of

Master of Science

in Engineering

at

The University of Wisconsin-Milwaukee

December 2017

ABSTRACT

CLINICAL NEAR-INFRARED SPECTROSCOPY INSTRUMENTATION: POSTURAL ORTHOSTATIC TACHYCARDIA SYNDROME STUDIES

by

Parvathi Kadamati

The University of Wisconsin-Milwaukee, 2017
Under the Supervision of Professor Mahsa Ranji

Aims: Postural orthostatic tachycardia syndrome (POTS) is a type of chronic orthostatic intolerance, annually affecting around 500,000 young Americans. Symptoms of POTS include lightheadedness and persistent increase in heart rate with upright body posture [1-3]. It requires a medical diagnosis. Impaired cerebral oxygenation of patients with POTS has been reported [4]. The pathophysiology remains unclear, and research is needed to understand the underlying conditions that lead to POTS. The aim of this research is to design a medical device called Cytoximeter and apply it to conduct a study between POTS patients and healthy controls for objective monitoring and quantitative measurements.

Introduction: A custom build near-infrared spectroscopy (NIRS) device called Cytoximeter was constructed to monitor the blood oxygenation and the redox behavior of intact tissue's Cytochrome C Oxidase (CCO), in clinical and research setting, noninvasively. The presence of hemoglobin absorption leads to complex algorithm implementation to separate the signals of the hemoglobin and CCO. Today we have different kinds of oximetry available, which provide information about the hemoglobin levels. However, the hemoglobin signals can only provide information regarding the changes of oxygen in the tissue. Monitoring CCO may give us information about the metabolic status of the tissue and intracellular levels of oxygen [5]. CCO is the final acceptor in the electron transport chain (ETC) and is an essential part of aerobic or anaerobic metabolism [3, 6]. CCO reduces by taking electrons in ETC cycle. This enzyme accepts electrons and changes to reduced

state. The custom build optical device is designed to monitor the optical densities of the tissue by applying Beer-Lambert's law to monitor the change in concentration of these chemicals. This ability can give the NIRS many applications for research and clinical purposes. POTS is a clinical application for this device; a study was conducted to monitor the POTS patients and healthy control subjects to observe the difference in oxygenation levels between these two groups while undergoing the head up tilt table test.

Methods: I measured and compared the difference in the changes in oxyhemoglobin and deoxyhemoglobin by applying this Cytometer to POTS patients and healthy controls while undergoing the heads-up tilt. The device uses the optimal source to detector separations to acquire the CCO signal and change in oxygenation of hemoglobin signals, which uses the six wavelengths near-infrared spectroscopic design. Validation of the device includes conducting the phantom studies and employing new experimental protocols. In the clinical setting, the device was applied to the muscles and brain tissue of the patients with POTS and Epilepsy under the standard care of neurological examiners.

Results: The results showed significant differences in deoxyhemoglobin, oxygenation change and blood volume between the control subjects and POTS patients. We found that the arterial system is less compliant with the inability to receive additional blood volume in POTS patients. Results of the phantom studies that I conducted showed that the device was able to monitor the real-time changes in oxygenation of blood and the redox state of CCO.

Conclusion: The custom build Cytometer successfully monitored the hemoglobin signal along with the CCO signal. The device provided an objective means of measuring and physiological findings in understanding the underlying reasons of POTS. Further work is required to determine whether the calf muscle activation of POTS patients is comparable to the healthy controls.

To
my parents,
and my husband,

TABLE OF CONTENTS

TABLE OF CONTENTS	V
LIST OF FIGURES.....	VII
LIST OF TABLES.....	IX
LIST OF ABBREVIATIONS.....	X
ACKNOWLEDGEMENTS.....	XI
1. INTRODUCTION.....	1
1.1 MY CONTRIBUTIONS	2
1.2 TISSUE OPTICS	4
1.3 PRINCIPLES OF NEAR-INFRARED SPECTROSCOPY	5
1.3.1 Oximetry.....	5
1.4 CELLULAR RESPIRATION.....	7
1.4.1 Hemoglobin.....	7
1.4.2 Cytochrome C Oxidase	7
1.5 CYTOXIMETER.....	8
1.6 MONTE CARLO SIMULATIONS	10
1.7 POTS	12
1.8 EPILEPSY	13
2. INSTRUMENTATION AND DESIGN	15
2.1 HARDWARE IMPLEMENTATION.....	16
2.1.1 Probe.....	17
2.1.2 Control Box.....	19
2.2 SOFTWARE IMPLEMENTATION.....	19
2.2.1 LabVIEW.....	19
2.2.2 Dark Current Correction	20
2.2.3 Ambient Pollution Correction.....	21
2.2.4 Baseline Acquisition.....	21
2.2.6 Force Plate Protocol Baseline	22
2.2.6 Acquisition VI	23
2.2.7 Offline Data Analysis.....	24
2.3 RESEARCH PROTOCOLS	25
2.3.1 Strain Gauge	25
2.3.2 Force Plate Apparatus.....	25
2.3.3 Pressure Cuff Validation.....	26
2.4 PHANTOM VALIDATION.....	27
2.4.1 Solid phantom	27
2.4.2 Phantom Experiments	29
3. CLINICAL DATA	31
3.1 POTS EXPERIMENTAL PROTOCOL.....	32
3.1.1 POTS Patients.....	33
3.1.1 Healthy Controls.....	34

3.2 EPILEPSY EXPERIMENT PROTOCOL.....	34
3.3 CLINICAL DATA	35
3.3.1 <i>POTS and Healthy controls Clinical data</i>	35
3.3.1.1 Validation of device	36
3.3.1.2 Physiological findings	37
3.3.1.3 Statistical differences.....	38
3.3.2 <i>Epilepsy Clinical data</i>	39
3.4 RESEARCH PROTOCOL RESULT	40
3.4.1 <i>Pressure Cuff Experiment</i>	41
3.4.2 <i>Force Plate Experiment</i>	41
<i>Conclusion and Discussion</i>	43
4. CONCLUSION AND FUTURE WORK.....	45
4.1 CONCLUSION.....	46
4.2 FUTURE WORK.....	46
BIBLIOGRAPHY	48

LIST OF FIGURES

Figure 1.1 The absorption spectra for oxyhemoglobin and deoxyhemoglobin	7
Figure 1.2 The absorption spectra of the four chromophores in NIRS region	9
Figure 1.3 The path of a single photon particle traveling inside the tissue	11
Figure 1.4 Monte Carlo simulations for muscle geometry.	12
Figure 2.1 Custom build NIRS Oximetry system.....	16
Figure 2.2 Cytoxiometer system.....	17
Figure 2.3 Probe head	18
Figure 2.4 Introducing the fiber optics and Laser diodes	18
Figure 2.5 Dark current front panel window	21
Figure 2.6 Baseline front panel window	22
Figure 2.7 Force Plate Protocol Baseline.....	23
Figure 2.8 Acquisition front panel window	24
Figure 2.9 The strain gauge protocol.	25
Figure 2.10 The Force plate apparatus.....	26
Figure 2.11 Pressure Cuff Protocol.....	27
Figure 2.12 Solid phantom.....	29
Figure 2.13 Phantom Results	30
Figure 3.1 The heads-up tilt table protocol.....	32
Figure 3.2 Image of the Tilt table Protocol.....	33
Figure 3.3 Epilepsy protocol.....	35
Figure 3.4 Results of Tilt table test.	35

Figure 3.8 Epilepsy representative monitored raw data.....	40
Figure 3.9 Pressure Cuff results.....	41
Figure 3.10 The results from a force plate experiment.....	42
Figure 3.11 The blood volume and change in oxygenation.....	43

LIST OF TABLES

Table 2.1 Optical properties of the phantom and simulated tissue.....	28
Table 3.1 Subjects details.....	34

LIST OF ABBREVIATIONS

CCO	Cytochrome C Oxidase
NIRS	Near-Infrared Spectroscopy
ETC	Electron Transport Chain
POTS	Postural Orthostatic Tachycardia Syndrome
Hb	Deoxyhemoglobin
HbO ₂	Oxyhemoglobin
MCW	Medical College of Wisconsin
CHW	Children's Hospital of Wisconsin
IRB	Institutional Review Board
VI	Virtual Instrument
DAQ	Data Acquisition
HUT	Head-up tilt table
HR	Heart rate
LED	Light-emitting diode

ACKNOWLEDGEMENTS

I thank my graduate advisor Dr. Mahsa Ranji for her guidance as well as for providing necessary information and the direction during my graduate studies. I would not have been able to accomplish this work without her supervision and commitment to excellence. I am grateful to work in the Biophotonics Lab during the past two years.

I also want to thank the staff of the Medical College of Wisconsin. I must thank Dr. Harry Whelan from Neurologist department of MCW for his expertise and enthusiasm. Dr. Whelan also helped me in promoting my research and connecting me with the professionals at MCW who made the clinical testing possible. I would also like to thank Dr. Brendan Quirk for supplying the chemicals and sharing knowledge required for this work. I am also deeply indebted to Dr. Thomas Chelimsky and Dr. Gisela Chelimsky from Children's Hospital of Wisconsin, who helped and shared knowledge for this study.

I am also grateful to the members of the Biophotonics Lab past and present. I wish to Jeffrey Sugar for their instrumental role in laying the groundwork for the device used in this study. I am also indebted to Shima Mehrvar who helped with regular reviews and input for my writings. Research of any kind would have been impossible without financial and organizational support, provided by the department in the form of TA funding.

I also much appreciate the support of my family and friends, especially my husband Satish Kumar Chipurapalli, my father Kadamati Appalaraju, my mother Kadamati Padmavathi and to my baby. Their understanding and support gave me the strength to keep going when I would have faltered.

Finally, I would like to thank the subjects who agreed to participate in this study. Without your willingness to give of yourselves, research and progress would stagnate.

Thank you all.

1. Introduction

Near-infrared spectroscopy (NIRS) is commonly used to monitor hemodynamic responses by the measuring of the regional concentration changes of oxyhemoglobin (HbO₂) and deoxyhemoglobin (Hb) using near-infrared light [1, 2, 6]. There is no risk or harm in applying NIRS to subjects for a long time. NIRS also has a high time-based resolution, portable, and low cost of equipment. These give NIRS many applications in clinical settings monitoring biological signals [7]. A variety of hemoglobin-based oximetry devices are available; however, clinicians currently cannot monitor the metabolic status of the tissue continuously and noninvasively [2, 8]. This research aims to monitor the cytochrome c oxidase (CCO) signal noninvasively by extending the optical techniques used in NIRS. CCO is an enzyme in the mitochondria which take place in electron transport chain (ETC) and hence can give information about the tissue metabolism [1, 2, 6]. Light in the NIRS transparency window can easily penetrate deep into tissue and can be utilized to monitor the changes in the concentration of absorbing chemicals inside the tissue. The challenge of this work lies in the measuring tiny CCO signal along with a significant value of hemoglobin in the tissue using NIRS.

Applying this clinical device to diseases like Postural orthostatic tachycardia syndrome (POTS) patients and Epileptic patients could provide an understanding to the clinicians about underlying reasons behind these disorders.

1.1 My Contributions

I developed and implemented a second-generation tissue Cytoximeter system based on the first-generation system developed in Biophotonics Lab. I then applied this method to study the difference in the change in Oxygenation of blood in POTS affected patients and healthy control subjects. In the procedure, the first step is to determine whether a healthy control subject has any

observable differences from the POTS patients. To show whether this Cytoximeter can detect the difference between POTS patients and healthy individuals. The results of this study between the POTS patients and healthy controls led to a journal article that is in the process of submission for publication and three poster presentations. One at the Institute of Electrical and Electronics Engineers (IEEE) Milwaukee, which was awarded the 3rd place in the graduate category, two in College of Engineering and Applied Science (CEAS) poster competition in 2016 and 2017.

I have redesigned the hardware of the Cytoximeter and replaced LEDs with LASER diodes of different wavelengths (705nm, 735nm, 750nm, 785nm, 808nm, and 850nm) and fiber optics system. The LASERs were employed as they have the tighter bandwidth and gives more collimated light. A new probe was designed using six different light sources with different wavelengths in the near-infrared window (650-1000nm). These wavelengths are chosen to be different from the previous incarnation of the probe as cross-talk between the chemicals was found in the results of the earlier version. I also introduced a fiber optic system which made the probe more efficient. The higher the number of wavelengths required for more advanced data processing protocol and filtering algorithm is needed. By using the new wavelengths and new data processing algorithms, the latest version of the Cytoximeter system can monitor the CCO along with the change in oxygenation of blood. In the making of second version Cytoximeter probe, I had to implement several novel approaches.

In this research project, I used different Computer-aided tools and programming languages. The device was controlled by a laptop running a LabVIEW program. The Virtual Instrument (VI) drives the device, displays and records the data in real time. I have designed a new LabVIEW experimental protocols. I have also made some changes in LabVIEW VI program to run the latest second version of cytoximeter. The recorded data was post-processed using a MATLAB

programming. I have made some changes to the MATLAB code, as the new version uses different wavelengths produced by LASER diodes as a light source. Post processing includes the extraction and separation of the CCO signal and hemoglobin signals. The graphing of representative signals.

As a validation of my probe, I have created a new experimental protocol using a force plate apparatus where the amount of force applied by the subject can be measured, and LabVIEW software can monitor the signal of the hemoglobin and CCO. Based on the previous phantom approach done by people in Biophotonics lab, I have implemented a similar experiment for validating the CCO signal for this new version of Cytoximeter. This ability could provide crucial diagnostic information by giving more information about metabolism than a standard blood oximetry device. The ability to detect metabolic activity status independent of blood oxygenation could help to determine different parameters of the disease quantitatively.

Since the study requires human subjects, I was certified by the Institutional Review Board (IRB). My responsibility includes editing and maintaining the consents, recruiting subjects and conducting every personal for the experiment. I was approved in the Institutional Animal Care and Use Committee (IACUC), and I am responsible for the IACUC protocol compliance as well.

1.2 Tissue Optics

The tissue oximetry uses a continuous wave light source incident on the tissue. The incident light migrates through the tissue. The amount of light and angle of light traveling inside the tissue entirely depends on the absorbing and scattering coefficients of the tissue. While considering the path of the incident light, one should assume the light traveling inside the tissue as light particles called photons. The photons travel through the tissue, and some of them are absorbed, and some diffuse reflected. An oximeter records change in the absorption along the path of photons through the tissue from source to detector [9]. These change in absorption are used to calculate

concentration by using Beer's law. The path must be determined to find the depth of penetration and find the concentrations using Beer's law. The determination of this path length is discussed in section 1.3 and its subsections.

1.3 Principles of Near-Infrared Spectroscopy

NIRS utilizes wavelengths in the near-infrared window (650-1000 nm) to determine *in vivo* concentrations of chromophores. A useful application of NIRS is to monitor the health and function of a biological tissue both noninvasively and non-destructively.

1.3.1 Oximetry

In the oximetry, near-infrared light is used to measure the changes in concentrations of oxyhemoglobin (HbO₂) and deoxyhemoglobin (Hb) via the modified Beer-Lambert law. This law relates the amount of light absorbed to the length of the path that the light travels and the concentrations of chemicals in the tissue [9]. There are two types of oximeter configurations one is transmission oximetry and other is reflection oximetry. In reflective configurations, the light source and detectors are placed on the same side of the tissue and the light that is observed at the detector has been scattered back from the tissue [10]. In transmission oximeters, the light and detector are placed on opposite sides of a thin tissue typically a finger or earlobe [12, 21]. In general oximetry, a source of light is incident on the tissue and this light penetrates inside the tissue traveling in a phase like absorption and scattering or reflecting the detectors [9]. In both systems, measurement includes the amount of incident light and detected light at the detector. Both forms depend upon the Beer-Lambert law to calculate chromophore concentrations. The Beer-Lambert law is as follows:

$$\ln\left(\frac{I_o(\lambda)}{I(t, \lambda)}\right) = \sum L_i \mu_{\lambda_i} \Delta C_i \quad (1.1)$$

Where $I(t, \lambda)$ is the light observed at the detector, $I_o(\lambda)$ is the expected or incident light at the detector, μ_i is the absorption coefficient of a given chemical, ΔC_i is the change in concentration of a given chemical and L is the average path length that the photon takes from the source to the detector. This equation is valid for all wavelengths λ although the absorption coefficients will vary with wavelength according to the absorption spectra of chemical 'i' [11-13].

These wavelengths are selected to give the highest signal to noise ratio (SNR). The oximeter typically uses wavelengths where the absorption spectra of the two species are very different [14]. Tissue oximeters often use two different wavelengths to determine the concentrations of both species of hemoglobin. Occasionally, oximeter uses a 3rd wavelength that corresponds to a point where the two wavelengths have very similar absorption coefficients [15]. This cross point is known as the isosbestic point and can be used to measure blood volume.

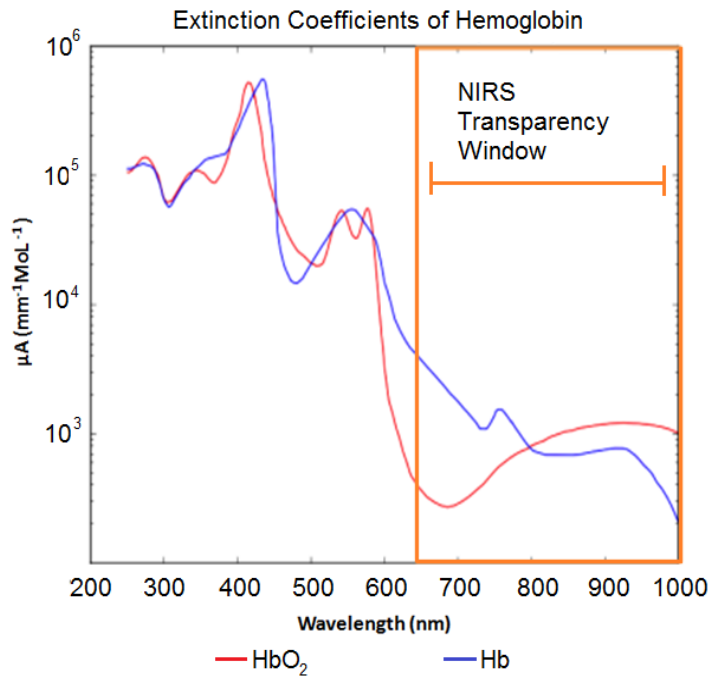


Figure 1.1 The absorption spectra for oxyhemoglobin (HbO₂) and deoxyhemoglobin (Hb). The window highlighted is the transparency window in NIRS, which tissue has the lowest absorption and is nearly transparent to light.

Figure 1.1 compares the absorption spectra of Hb and HbO₂. When hemoglobin attaches or detaches from oxygen, it undergoes a small conformational change that causes a slight difference in absorption spectra.

1.4 Cellular Respiration

Cellular respiration consists a large chain of reactions and metabolic activities that take place in the cell of the living organisms. The term includes both aerobic and anaerobic respiration, and the energy is generated during this process with oxygen and without oxygen respectively. If monitoring oxygen consumption, it is giving the information about the tissue's aerobic cellular respiration; it does not include any information about anaerobic cellular metabolism. So, monitoring Cytochrome c oxidase may provide information on anaerobic metabolism [5, 6, 16].

1.4.1 Hemoglobin

Hemoglobin is the oxygen transport protein in the red blood cells. As it carries oxygen, hemoglobin is involved in aerobic metabolism. This metabolism requires both oxygen and glucose to function. The oxygen that fuels the aerobic metabolism is the oxygen molecules that are separated from HbO₂ particles. Once it gives the oxygen molecule, it changes to Hb. By monitoring changes in oxyhemoglobin and deoxyhemoglobin, the aerobic metabolism can be obtained [5, 16].

1.4.2 Cytochrome C Oxidase

Cytochrome c oxidase (CCO) is transmembrane protein found in mitochondria of the cell. To understand the CCO NIRS signal, one must know the biochemistry behind it. CCO is the final acceptor ETC. The mitochondrial ETC mediates several different transfers, in the process

converting ADP to ATP. The change in ATP/ADP ratio provides usable energy to drive a wide variety of cellular processes [6, 17].

As the final acceptor, CCO accepts the electrons at the end of ETC. When it does, it changes to reduced state. Then CCO oxidizes and uses the energy produced to pump the protons across the cell membrane. This process happens very quickly and slowly compared to ETC process as a whole. So, monitoring the CCO redox state by expecting more reduced state in metabolic activity and may give information of anaerobic metabolism [15, 18].

1.5 Cytoximeter

The cytoximeter is designed to obtain both the hemoglobin signal and CCO signal in the selected region of the tissue. The exact wavelengths must be chosen to estimate the amount of CCO in the tissue based on the absorption spectrum. Like hemoglobin changes whether associated or dissociated with an oxygen molecule, CCO undergoes a similar conformational change that affects its absorption spectra as the molecule reduces or oxidizes [19]. The same method that tracks the changes in HbO₂ and Hb has been extended to monitor CCO by adding additional wavelengths to the detection device. By using all six wavelengths to find the concentrations of the four chemicals as noted in the figure. In the previous version of Cytoximeter different wavelengths were used and in results they found cross-talk between four chemicals- HbO₂, Hb, reduced CCO (cyt red) and Oxidized CCO (cyt ox). So, to negate the cross-talk between these chemicals, a simulation of the wavelengths in the Infrared region (IR) of the absorption spectra was executed and new wavelengths were determined. The optimum wavelengths determined were 705nm, 735nm, 750nm, 785nm, 808nm, and 850nm. Figure 1.2 shows the absorption spectra for all four chemicals monitored in this study.

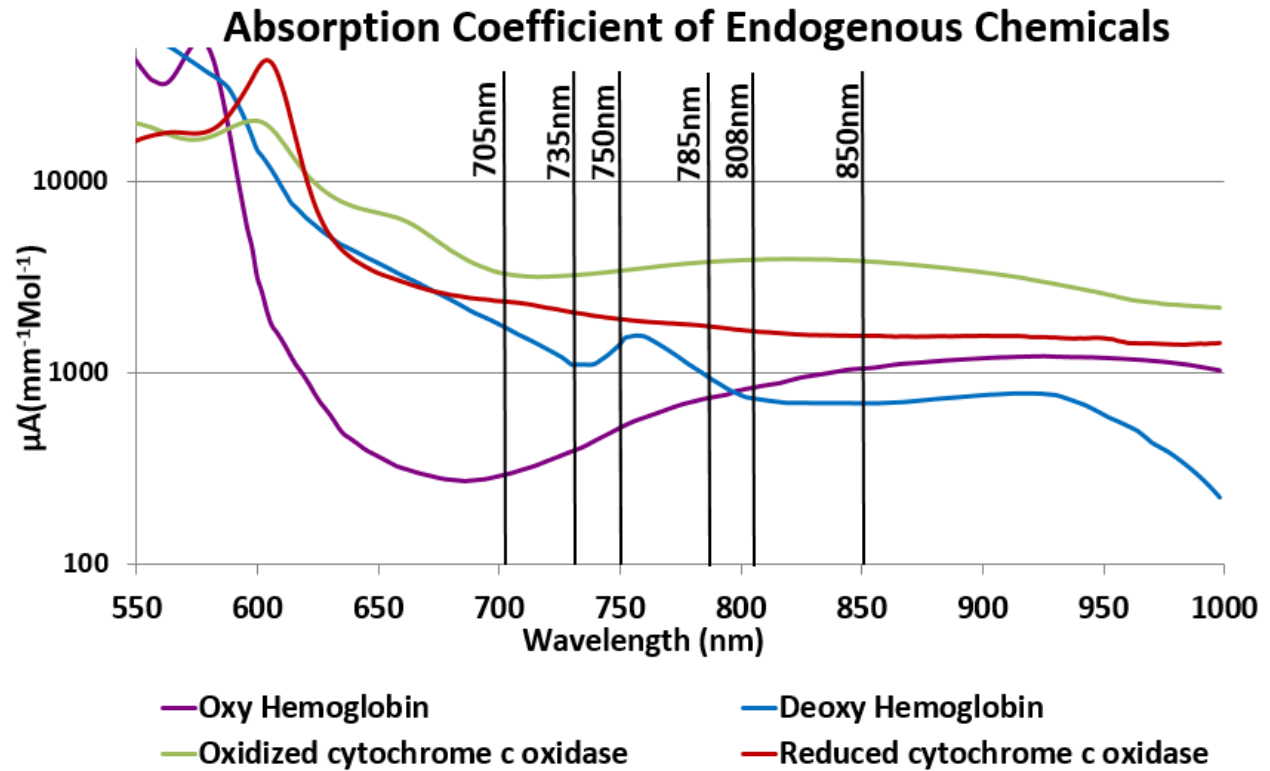


Figure 1.2 The absorption spectra of the four chromophores in NIRS region. The six wavelengths that are used to identify these chemicals are highlighted by black lines.

CCO will not account for most of the light absorption at any of these wavelengths [15]. Therefore, it is necessary to cancel out the effects of the hemoglobin on absorption before calculating the amount of cytochrome in the tissue. The following equation allows the extraction of the concentration of these four parameters:

$$\begin{pmatrix} \Delta OD_{705} \\ \Delta OD_{735} \\ \Delta OD_{750} \\ \Delta OD_{785} \\ \Delta OD_{805} \\ \Delta OD_{850} \end{pmatrix} = L \begin{pmatrix} \mu_{Cyt\ ox}(705nm) & \mu_{Cyt\ red}(705nm) & \mu_{Hb}(705nm) & \mu_{HbO_2}(705nm) \\ \mu_{Cyt\ ox}(735nm) & \mu_{Cyt\ red}(735nm) & \mu_{Hb}(735nm) & \mu_{HbO_2}(735nm) \\ \mu_{Cyt\ ox}(750nm) & \mu_{Cyt\ red}(750nm) & \mu_{Hb}(750nm) & \mu_{HbO_2}(750nm) \\ \mu_{Cyt\ ox}(785nm) & \mu_{Cyt\ red}(785nm) & \mu_{Hb}(785nm) & \mu_{HbO_2}(785nm) \\ \mu_{Cyt\ ox}(805nm) & \mu_{Cyt\ red}(805nm) & \mu_{Hb}(805nm) & \mu_{HbO_2}(805nm) \\ \mu_{Cyt\ ox}(850nm) & \mu_{Cyt\ red}(850nm) & \mu_{Hb}(850nm) & \mu_{HbO_2}(850nm) \end{pmatrix} \begin{pmatrix} \Delta C_{Cyt\ ox} \\ \Delta C_{Cyt\ red} \\ \Delta C_{Hb} \\ \Delta C_{HbO_2} \end{pmatrix} \quad (1.2)$$

This equation is the form of a constrained regression problem. This problem can be solved by a Penrose pseudo-inverse to each side of the equation to be left with an estimate of the concentrations of the absorbing species on the right-hand side of the equation. While this method would work under ideal conditions, in practice there are several numerical problems often arise from approaching a problem such as this. By considering six wavelengths, a few co-linearity problems will be introduced into the regression matrix. All these issues were solved in the previous version of Cytometer [13].

1.6 Monte Carlo Simulations

The optimal distance between the source and detector depends on the structure of the tissue; the wavelengths used and desired depth of penetration. Increasing the source to detector separation results in greater depth of penetration [20]. But increasing the separation distance decreases the signal to noise ratio. A Monte Carlo method is applied to choose the optimal source-detector separation for the geometry of calf muscle oximetry. Monte Carlo is a stochastic process that models the path of photons through the tissue by repeated simulations [21, 22]. Every single

photon particle will undergo several scattering events in its propagation path from the incident point to the detection side as a step path as shown in the fig. 1.3. This step size for single photon can be determined by equation 1.3,

$$\Delta s = \frac{-\ln(\xi)}{\mu_t} = \frac{-\ln(\xi)}{\mu_s + \mu_a} \quad (1.3)$$

Where ξ is a random variable between 0 and 1, μ_a is the absorption coefficient, and μ_s is the scattering coefficient.

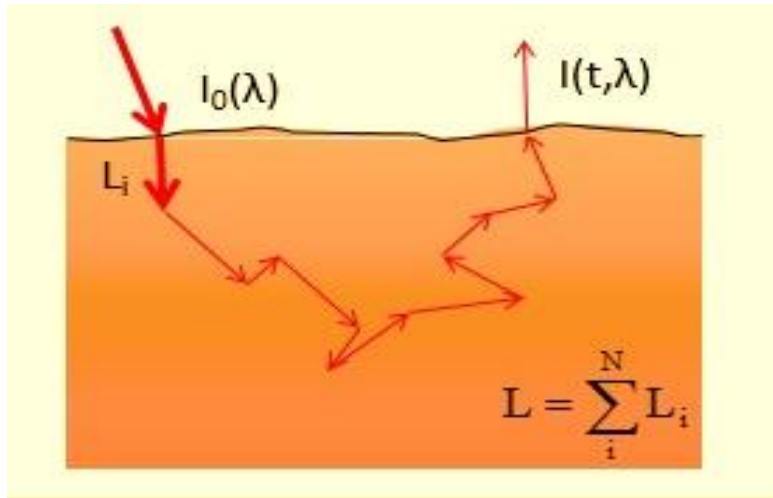


Figure 1.3 The path of a single photon particle traveling inside the tissue. After being scattered multiple times. The photon leaves at the same plane it was injected.

By using Monte Carlo simulation, a computerized program is designed to process millions of photons while the undergoing absorbing and scattering at multiple layers of simulated tissue. The simulation was coded in a C++ environment, and image processing is performed with MATLAB by members in Biophotonics lab. The results of these simulations are displayed below. The tissue is modeled by 0.3 mm of the dermis, 1 mm of sub-dermis and a semi-infinite layer of the muscle beyond. Fig. 1.4 and 1.5 show Monte Carlo simulation results of light penetration in the tissue for 2 cm and 3 cm source to detector separation obtained by simulating the trajectories

of 10^8 photons through the calf and brain tissue. The densest parts of these simulations are graphed to give a sense of the average penetration of this optical path. The 2 cm source to detector separation provides a depth of penetration up to 1 cm. The 3 cm source to detector separation gives a depth of penetration up to 1.5 cm.

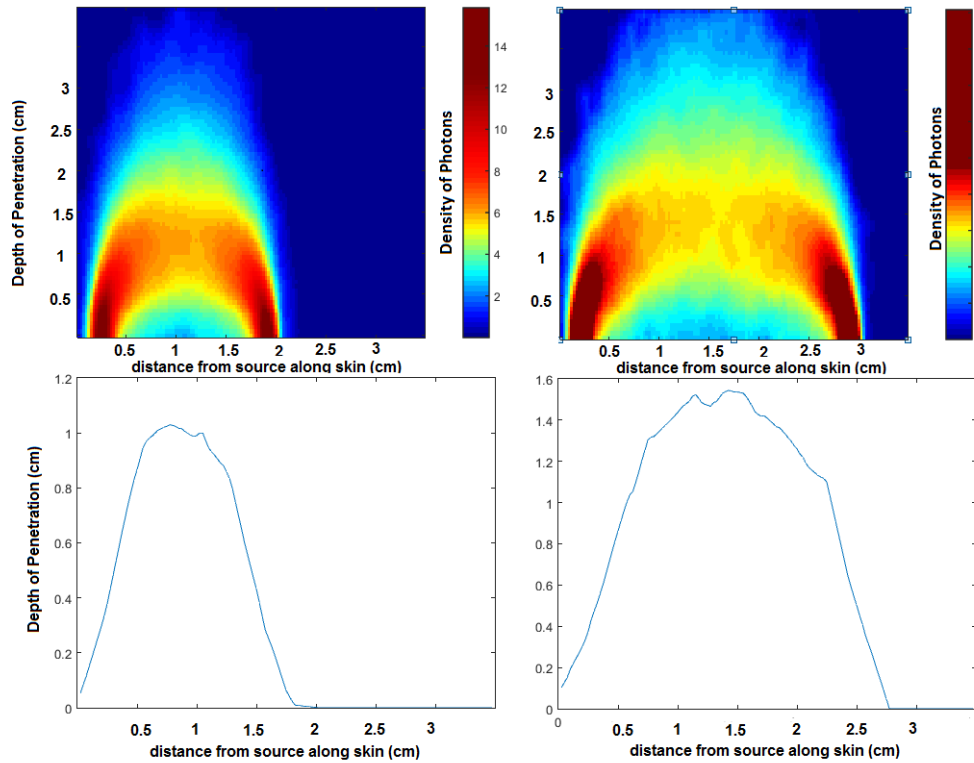


Figure 1.4 Monte Carlo simulations for muscle geometry at both 2 cm and 3 cm source-detector separations. The densest parts of these simulations are shown on the bottom row to give a sense of the average penetration of these optical paths.

1.7 POTS

Postural orthostatic tachycardia syndrome (POTS) is a syndrome caused by the postural changes in the body of the patient with POTS. Symptoms of POTS include lightheadedness and persistent increase in heart rate (> 30 bpm in adults and > 40 bpm in children) with upright body posture [1-3]. Patients with POTS may experience many other symptoms such as fatigue,

sweating, tremor, anxiety, palpitation and exercise intolerance. Recumbency and assuming a supine position typically improve symptoms; however, these symptoms may lead to a high level of functional disability [23, 24]. A wide range of medications and treatment strategies are available, mainly emphasizing volume expansion and exercise [23].

In this study, muscle oxygenation and metabolism of POTS patients were monitored to assess the effect of the postural change during Head-up tilt table (HUT). HUT is a standard test for patients with a potential POTS diagnosis to evaluate their response to postural change. During the HUT, blood pressure and heart rate are measured continuously [25]. However, subjects with an increase in heart rate that meets the diagnostic criteria for POTS have the same symptoms as those who do not [26]. Thus, other physiologic abnormalities may be present, such as changes in brain or muscle perfusion that might be detectable with a device such as NIRS during an absence of other vital sign changes.

1.8 Epilepsy

Epilepsy may occur due to a genetic disorder or by attained brain injury, like trauma or stroke. Epileptic seizures have the disorder mostly in childhood neurologic condition and it a significant public health concern [8, 27]. The seizures cause poor coordination and disturbance of the different systems in the body and may even disable and interfere with the child's ability to learn, can also lead to harmful effects in social and psychological function [14, 28, 29]. When a seizure occurs, a person has symptoms and experiences like abnormal behavior, symptoms, sensations, and sometimes even have loss of consciousness.

Epilepsy is treated with medicines, and if it is a severe case it is treated by surgery, devices, or dietary changes. Epilepsy is a disorder in the nerve cell activity in the brain requires a medical

diagnosis and constant monitoring. NIRS technology has been used to monitor cerebral oxygenation and blood flow in children and adults in diverse conditions [30-33].

2. Instrumentation and Design

The Cytoximeter was designed to monitor the blood hemoglobin signal along with the CCO signal. The updated version of the probe has six different LASER sources and four photodetectors. LASERs were used in this new version as they have the tighter bandwidth and produce the more collimated output of light. This chapter gives the details of the device's design and instrumentation involved.

2.1 Hardware implementation

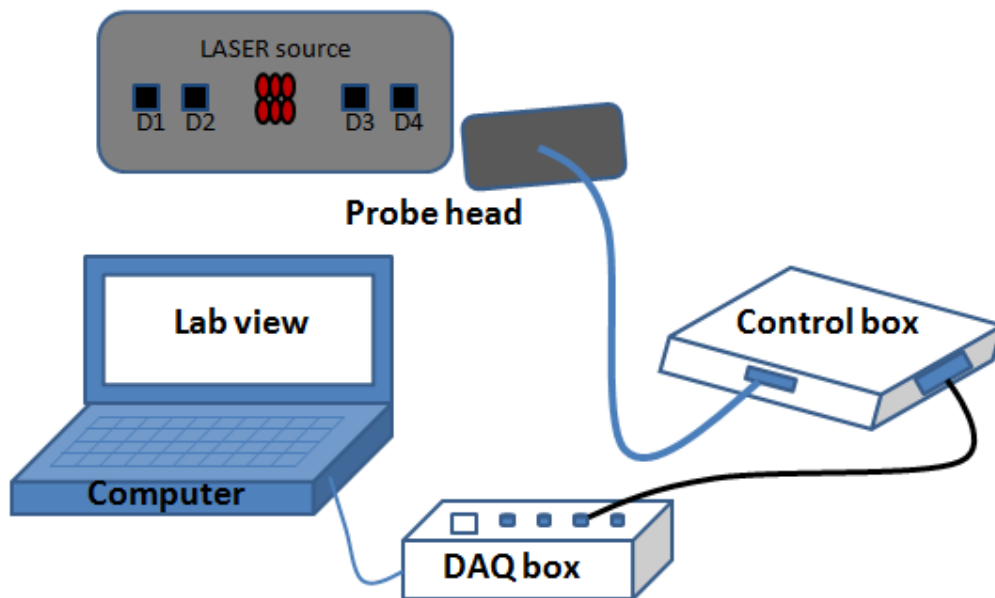


Figure 2.1 Custom build NIRS Oximetry system consists of control box and probe, connected to a DAQ box and a laptop to run Lab VIEW software.

Figure 2.1 shows the Cytoximeter schematic setup. The device is custom-made for this project that has a probe and a controlling box. The probe contains the light sources and detectors that are used to measure the optical densities of the tissue. The probe was placed upon the surface of the muscle or skull. The control box contains circuitry for controlling the components like detectors and turning the LASER diodes on and off in sequence. The DAQ board acquires the data

and records on the laptop. The laptop also displayed the results of the CCO and hemoglobin data in real time.



Figure 2.2 Cytometer system consists of DAQ board, control box, computer LabVIEW software and probe.

2.1.1 Probe

The probe head (figure 2.3) has the source and detectors, which are capable of producing and detecting six separate wavelengths of light. The light sources are LASER diodes. With different wavelengths 705, 735, 750, 785, 808 and 850nm (HL7001MG / HL7302MG / LT031MD / L785P5 / L808P010 / L850P030, Thorlabs inc., NJ., USA). An optical fiber is attached to each LASER (figure 2.4), and all these six fibers are presented at the center of the probe head. The optical fibers are used as the LASER diodes diameter is big and there are assembled in an area around 3x2 mm. Which make the source to detector separation variable, i.e., a different LASER to detector distances. So, to center them at a single point on the tissue, optical fibers are the best choice. The construction of probe head with fiber is shown in figure 2.4. On the detection side,

four multi-pixel photon counters (MPPC's) (Hamamatsu, S1133-14, Kyoto, Japan) were used on either side of the probe. These detectors were organized in two pairs to provide two different depths of penetration. The first pair of detectors were placed at a source-detector separation of 2 cm. The second pair of detectors were placed at a distance of 3 cm. As discussed in the previous chapter, the different source-detector separations produced different depths of penetration of the light.

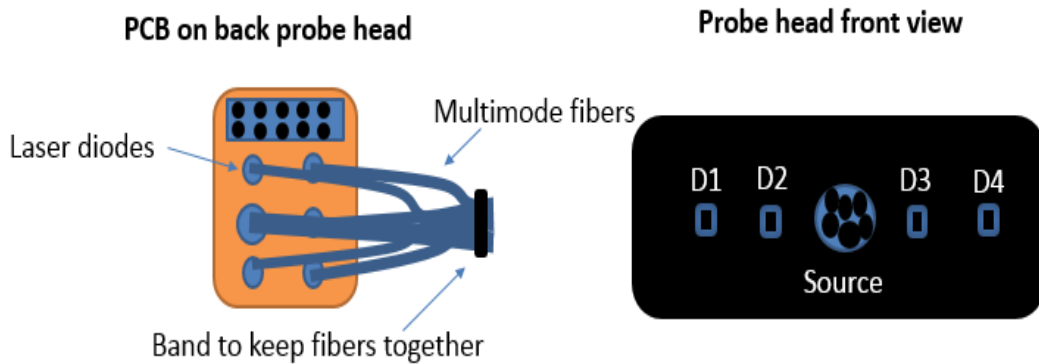


Figure 2.3 Probe head with four detectors and six different wavelengths LASER source (705/735/750/785/808 & 850nm)

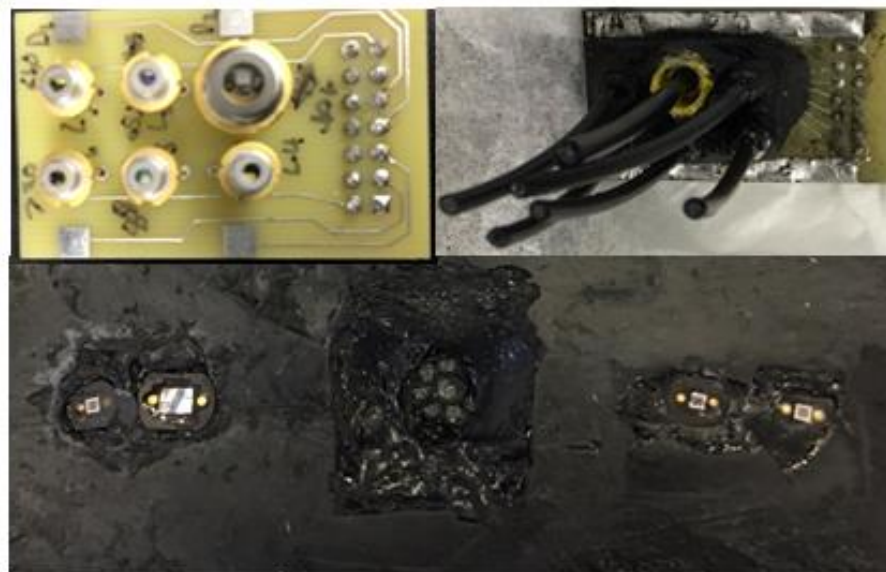


Figure 2.4 Introducing the fiber optics and Laser diodes. The figure shows the step by step construct process of the probe head.

2.1.2 Control Box

The control box which controls the probe head to detector the signal from detectors and to power the sources. It contains the amplifiers for the signal that comes back from the detectors on the probe. It also circuitry that drives for LASERs. The control box talks with the DAQ board on the analog and digital channels of the DAQ board. The LASER's were turned on and off by transistors in common emitter mode in the control box circuitry. These transistors were controlled and driven by the digital output from the DAQ board.

2.2 Software Implementation

The second version Cytoximeter software and implementation as the previous version. This section will give details for information LabVIEW program that helps to collect and monitor the data.

2.2.1 LabVIEW

The LabVIEW software operates the controlling parts of the Cytoximeter, like the DAQ board and circuit box. The software has a virtual instrument (VI) that accepts the analog input channels from the DAQ board for four detectors. Output a single eight-bit digital number to control which LASER to on and off based on configuration designed. The complete program was built with a large number of sub-Vis. Each sub-VI could perform its task and function that was necessary to the data analysis process. These sub-VIs was accessed through a top-level hub VI that also controlled the paths and names of the files generated by each sub VI. All of these VIs saves and store their data in a Technical Data Management Stream (TDMS) file format for post-processing.

The DAQ board was programmed to continuously sample at each of the channels at a fixed rate. This rate of sampling was obtained based on the maximum response time of the circuitry.

Similarly, the lights were turned on and off at a variable rate of up to 20Hz. That translates to a range of samples per wavelength and sampling rate for an entire six wavelengths cycle which can be changed depending on the results.

2.2.2 Dark Current Correction

The first VI in the series was the dark current correction VI. This VI get the amount of signal that was due to dark current on each of the channels. Dark current is an issue in every optoelectronic system which is caused by current leakage of the semiconductors in the detectors and by parasitic connections between the components in the system. As this process was not repeated before the experiment, subsequent VIs use the most recently obtained values. This test was done while the LASER's were being switched on but the board was placed on a black media.

This sub-VI is run before perform the main sub-VI, as it is essential to run while acquiring the small signals, as it may make a huge difference. The first VI in the series was the dark current correction VI. Dark current is a small little voltage that comes in the electronic system even when there is no light at the detectors. The dark current values were obtained to be stable over a long time and repeated tests. Therefore, it was assured that small changes in dark current were a minimal source of error in the system.

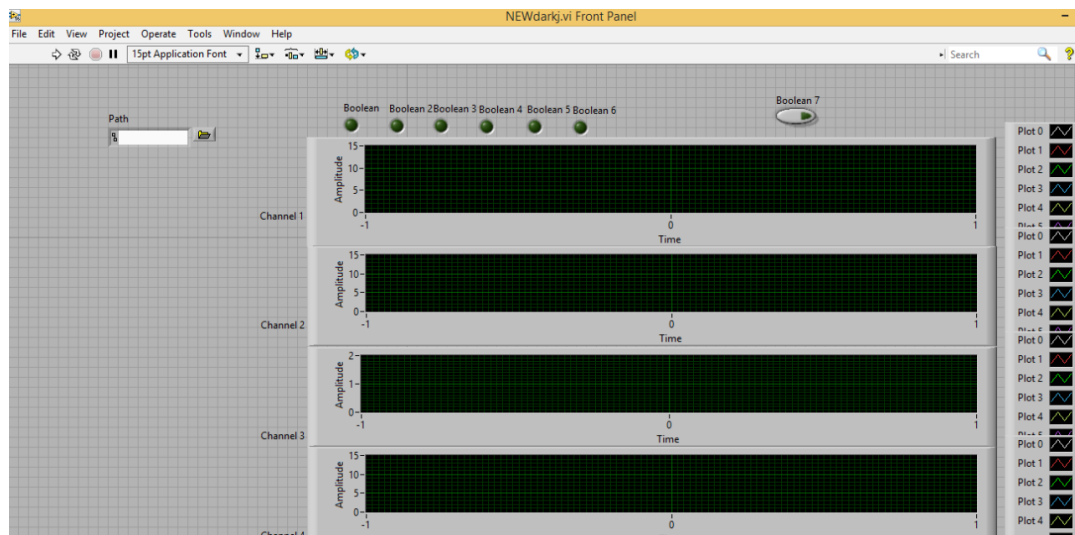


Figure 2.5 Dark current front panel window

2.2.3 Ambient Pollution Correction

To correct the ambient light pollution, a second sub-VI measured light seen by the probe after it had been applied to the subject. The LASER's were not switched on during this procedure so that only the ambient light was recorded during this time. Even though the detectors were located on the underside of the probe when it was applied to the subject's skin the detectors were sensitive enough to get the ambient light around the room with bright lighting. As the probe was designed for clinical use, it was considered that the lighting conditions in the room would not always be ideal.

2.2.4 Baseline Acquisition

To obtain optical densities baseline had to be processed and established. Except for the sources, i.e., LASERs, we do not want any other light affecting the baseline, so the dark current and ambient light levels which we obtained before baseline get subtracted from the baseline values. That was done by the baseline sub-VI internally. The baseline measurements were monitored until they were stable for at least a minute. The third VI obtains the baseline, during at the time where the LASER is not turned on or doing anything else to acquire the Hemoglobin signal and CCO signals.

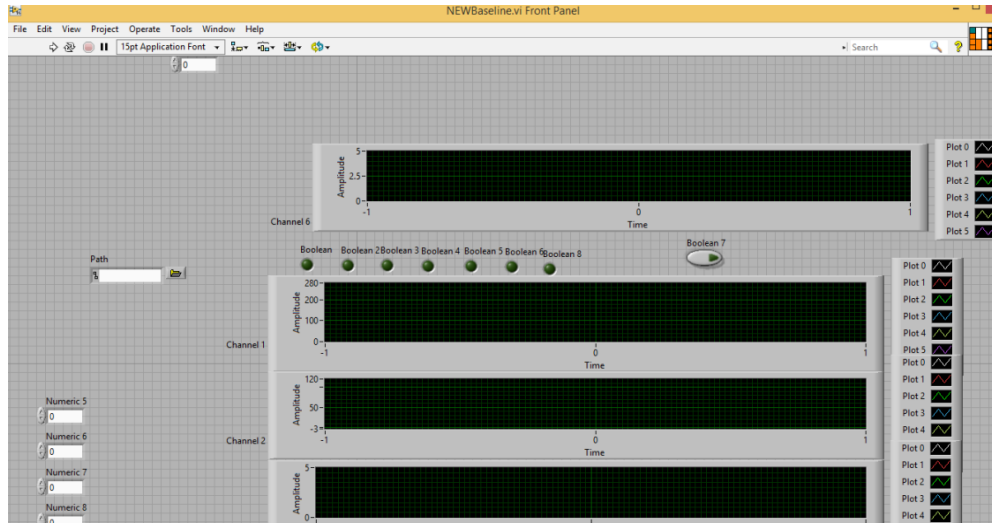


Figure 2.6 Baseline front panel window

2.2.6 Force Plate Protocol Baseline

In Force plate protocol, subject applies a force which is measured by the strain gauge. So this strain gauge instrumentation is connected to the LabVIEW software. In this, the subject needs to apply his/her maximum force at the starting of the experiment. So the LabVIEW software VI is designed to fix the maximum and then run the baseline VI to acquire the signals. This force plate baseline begins after the dark current VI. Once the maximum range of force is fixed in the VI, then baseline VI runs the LASERs and acquires the light levels. According to different protocol design, the subject may ask to apply certain of force (example 80%, 60% and 40% of max). While the baseline VI is in the process, when the subject applies certain force, it can record the value of the force applied.

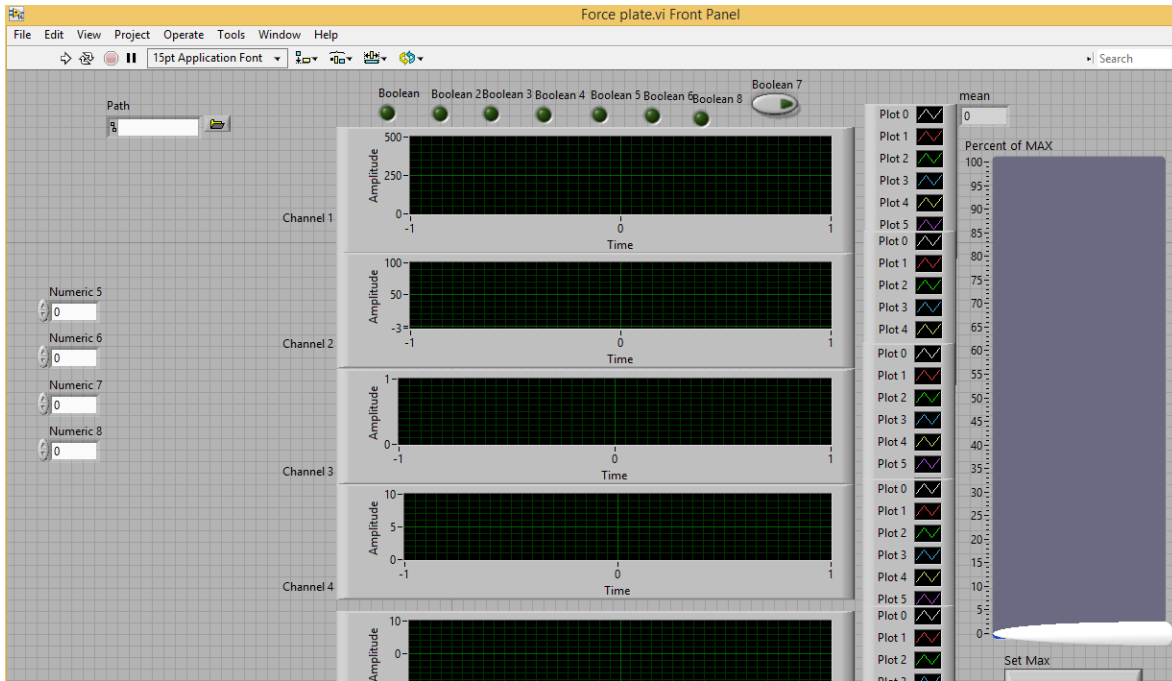


Figure 2.7 Force Plate Protocol Baseline

2.2.6 Acquisition VI

The acquisition VI was used for reading the light levels of the light the incident on the subject body and then it will change or convert them to optical densities. Then it will record and display the real-time estimates. The OD values are used to estimate the changes in hemoglobin and CCO values. The baseline VI was the first VI for the experiment. This VI can also perform the functions by subtracting the dark current and ambient light from the light levels obtained and then applying the modified Beer-Lambert law to get the signal changes.

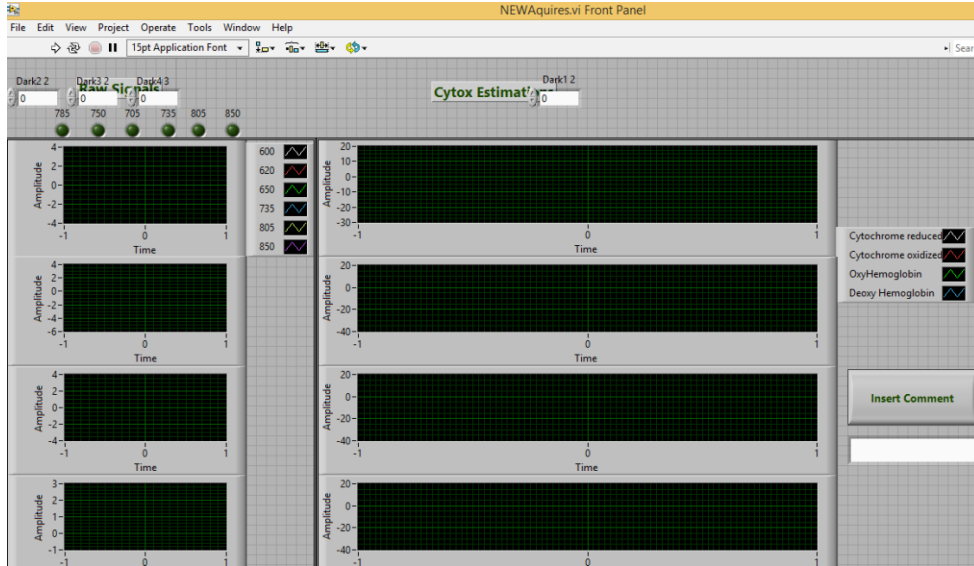


Figure 2.8 Acquisition front panel window

2.2.7 Offline Data Analysis

This code analyzed the information by performing a data analysis technique known as Kalman filtering, which is discussed and implemented in the previous version [13]. When the Kalman filtering algorithm was applied and completed, estimates of the trends of HBO₂, HB, Oxidized CCO, and Reduced CCO are obtained. In addition to these four signals, other three important signals were calculated, and these are blood volume, change in oxygenation (Δ oxy) and CCO redox state. These equation mentioned below are assumed approximations that give the general trend of the Δ oxy, CCO Redox State, and Blood volume. The Δ oxy, blood volume, and redox state were assumed estimations from the following equations.

$$\Delta oxy = \Delta C_{HbO_2} - \Delta C_{Hb} \quad (2.1)$$

$$\Delta BV = \Delta C_{Hb} + \Delta C_{HbO_2} \quad (2.2)$$

$$\Delta CCO \text{ Redox State} = \Delta \text{Reduced CCO} - \Delta \text{Oxidized CCO} \quad (2.3)$$

Reasonable expectations of Δ oxy would represent the ratio of HbO₂ to whole blood, Blood Volume would have the total blood in the tissue and redox state would represent the ratio of

reduced CCO to total CCO. As the device can only detect relative changes of these four chemicals and not the absolute values, which are impossible. So, the above equations are estimates of those chemicals. The data is collected and recorded in TDMS file format for post-processing. The TDMS file will open as excel format on a personal computer where the post analysis of the data is done. And then analyzed in MATLAB for processing and graphing of these chemicals.

2.3 Research Protocols

To understand and correlate the results of the custom build probe, some research protocols are employed. These protocols aimed to undergo some exercises. Designed a measuring apparatus using six-axis strain-gauge.

2.3.1 Strain Gauge

A six-axis strain gauge (Advanced Mechanical Technology, Inc., MC3A-1000, Watertown, MA) was utilized to measure the force that a subject applied to their foot Fig. 2.8. For the usage, applied the same settings and amplifier equipment that we used by the previous Biophotonics lab members.

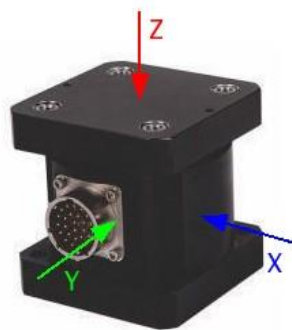


Figure 2.9 The strain gauge, arrows indicate the default coordinate system.

2.3.2 Force Plate Apparatus

A custom-built device was developed to hold the strain gauge in all these arrangements. This device can be seen in figure 2.9. The employed protocol required the capacity to get the drive that subjects were able to apply by flexing their foot while in

standing, inclined and sitting stances. This made the strain gage a challenging matter since the device had to be able to be utilized in all these arrangements. The apparatus was built from machined metal parts and lumber. The device also included a foot restraint that is commercially accessible for utilize in paddling work out machines.



Figure 2.10 The Force plate apparatus, designed to hold the strain gauge which measure the force applied by the subject.

2.3.3 Pressure Cuff Validation

A different approach, causing ischemia in the forearm muscle to validate the hemoglobin signals changes monitored by Cytometer. That was based on published research which uses a charge-coupled device (CCD) based tissue spectroscopy [36]. The same experimental protocol was applied to an individual to cross-checked the hemoglobin results of the Cytometer.

The probe was applied to the forearm muscle, and a pressure cuff is attached to the arm. By applying pressure rapidly to cause oxygen desaturation in the forearm as shown in the figure 2.11.



Figure 2.11 Pressure Cuff Protocol

2.4 Phantom Validation

2.4.1 Solid phantom

An artificial tissue called as phantom has two phases i.e., solid and liquid phase. The solid phantom was made by using 1% by mass agarose-gel [34]. The liquid phase consists of intralipid as scattering material and India ink as absorbing the material. The ink was used as it has the absorbing properties which could mimic different tissues [35]. The fat emulsion called intralipid was added as scattering coefficient to the gel with excellent reliability [34, 35]. Cubbedo reported on trends on optical properties using these materials. The data from these trends were used to create several layers of the phantom that resembles different layers of the tissue. The ink has a non-negligible contribution to scattering of the phantom to develop a more reliable phantom,

concentration of both Intralipid and India ink were extrapolated from writing that utilized a phantom that contained both [34, 36], that were used to change the optical properties of the gel.

The concentration of both India ink and Intralipid are added to the phantom based on the type of tissue. Different types of tissues have a different kind of absorption and scattering coefficients.

Tissue	Reduced scattering coefficient (cm^{-1})	Concentration of intralipid (% emulsion)	Absorption Coefficient (cm^{-1})	Concentration of India Ink by (% by volume) 10^{-5}
Dermis	23	3.2	0.02	3.6
Muscle	9.0	1.1	0.05	8.2
Skull	30	4.3	0.02	3.6
Brain	10	1.25	0.05	8.2

Table 2.1: Optical properties of the phantom and simulated tissue.

In the construction of the artificial tissue called phantom, which is made by mixing the agarose with water and heated in a microwave and then it cools down into a solid clear material. Then based on the tissue absorption and scattering coefficients India ink and intralipid concentrations are added as a solution. Thus, a layered solid phantom is made and be shown in the fig.2.10. a). The second phantom mentioned liquid phantom is made to detect the changes in concentrations like CCO, blood concentrations. To this liquid phantom, this concentration is added based on the tissue. So, to monitor this change liquid phantom is made. The phantom was constructed in a plastic cell culture flask (VWR cell culture flask, Standard Line, 75ml). An agarose gel layer was embedded on one side of the flask while the remaining volume of the flask is left empty. The rest of the flask was filled with a DI water, Intralipid and India ink solution that resembles the deeper tissues optical properties. The two-phase phantom is shown in figure 2.10 b).

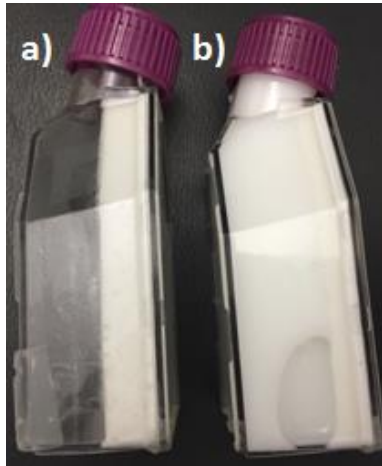


Figure 2.12 a) It is only a Solid phantom which is embedded and dried in the cell culture flask and stuck to the flask wall. b) Solid phantom filled with the liquid phase.

2.4.2 Phantom Experiments

The two-phase phantoms were used to test and detect the performance of the probe by detecting the change in concentration of CCO bolus. Figure 2.13 shows the results of one of the phantom test conducted. The probe is applied to the phantom and monitored the data by adding hemoglobin and CCO at different intervals. To monitor the reduction in this chemical's concentration, a reducing agent called Sodium Dithionite (Sigma-Aldrich, USA) is added. This experiment is done in a dark environment. The hemoglobin used was Ferrous hemoglobin from bovine blood (H2500, Sigma-Aldrich, USA). The cytochrome c oxidize chemical used for this study was prepared and test by MCW personal. The baseline was monitored without adding any of CCO or hemoglobin chemicals. In second interval, hemoglobin bolus is added where oxyhemoglobin signal showed an increase. In third interval, more hemoglobin bolus is added, oxyhemoglobin signal showed a step increase. Then in the next two interval CCO bolus added,

oxidized CCO showed rise and reduced CCO showed drop. And then a reduced by a reducing agent as sodium dithionite and monitored for around 10 minutes. Once the reducing agent came into action, slowly oxyhemoglobin and oxidized CCO decreased and reduced CCO increased. These results showed that the Cytosimeter device is able to monitor this chemical concentration changes.

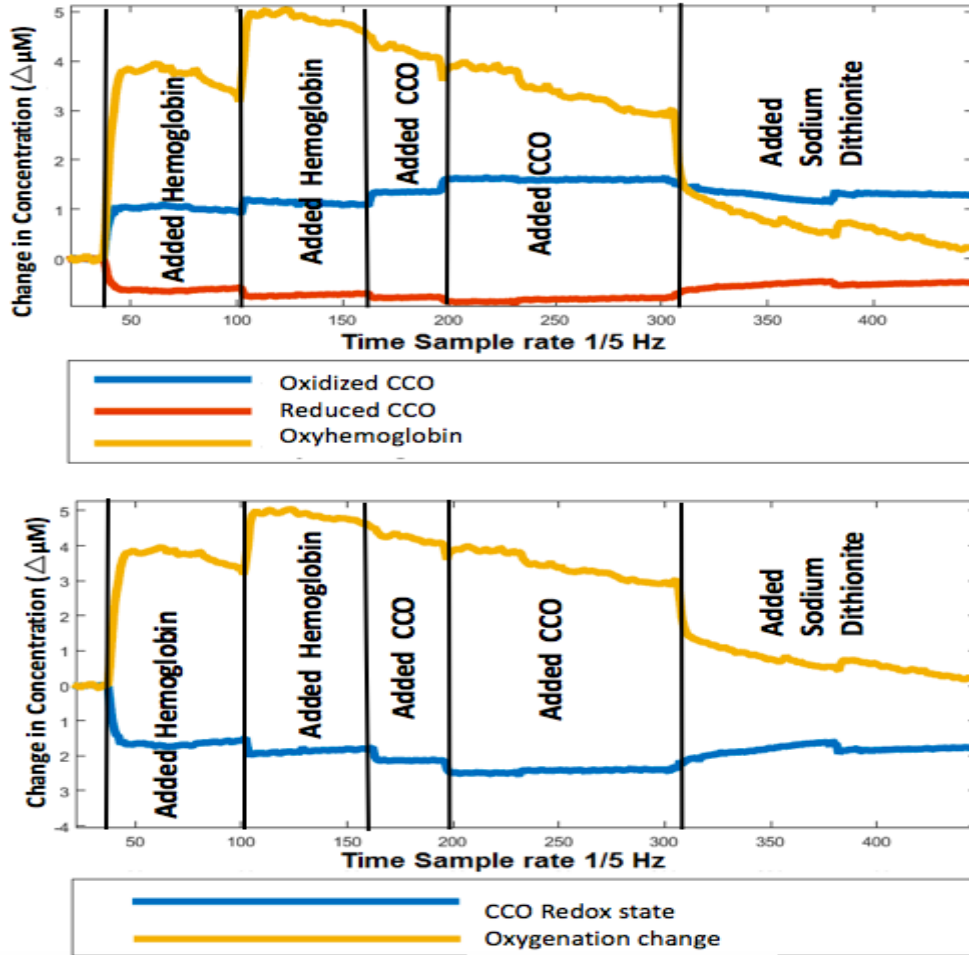


Figure 2.13 Phantom Results

3. Clinical Data

3.1 POTS Experimental Protocol

The NIRS oximetry probe was placed on the right gastrocnemius. A gold standard Covidien oximetry probe (INVOS 5100B, Covidien/Medtronic, Minneapolis MN, USA) was placed on the left gastrocnemius to be used as a reference for comparison of the change in oxygenation measurements Fig 3.2.

The subject is asked to lay on the tilt table, monitored for 10 minutes at 0° angle of the HUT as a baseline. And subject was taken to an angle of 70° and monitored for 30 minutes, and as a recovery for 10 minutes subject was reclined to 0° as shown in Fig 3.1.

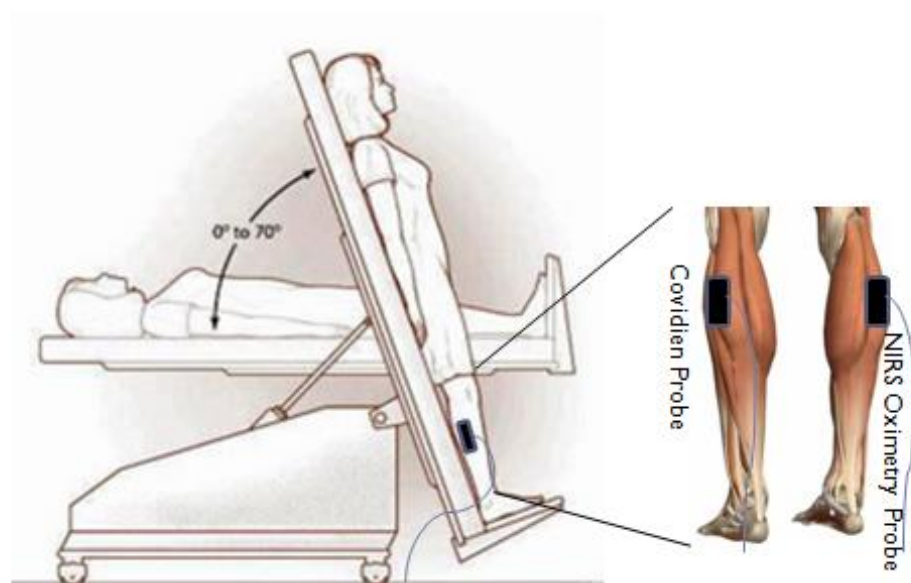


Figure 3.1 The heads-up tilt table protocol, NIRS oximetry probe and Covidien probe are attached to the gastrocnemius muscle. Monitor at 0⁰ and 70⁰ angles of the tilt table for 10 minutes and 30 minutes respectively.



Figure 3.2 Image of the Tilt Table Protocol

3.1.1 POTS Patients

All the POTS patients were recruited under the approval of Institutional Review Board in Medical College of Wisconsin and Children's Hospital of Wisconsin. All data were collected in Children's Hospital of Wisconsin, Wauwatosa, WI. As part of this exam, the patients were subjects to undergo heads up tilt table test. Twelve patients (age 8-18 years) underwent this protocol and were divided into 6 that completed the protocol who had POTS (rise in HR > 40 bpm in first 10 minutes) and 6 with syncope, and therefore had an incomplete tilt test and may or may not have had POTS.

The tilt table setup is shown in figure 3.1. On one leg our probe was placed and on the other leg, a commercially available oximeter was placed on the calf. The two devices were run in parallel while the subject underwent a 70° tilt for 30 minutes. This test was designed to exacerbate symptoms that the subjects were experiencing. Because of this condition, n=6 of tests were ended early because the subjects either fainted or were in too much discomfort to continue. As a result, n=6 of the subjects' data were counted in data processing for this experiment.

Subject type	Mean age \pm SD	Gender	Max HR first 10' of tilt	Max HR During Tilt (bpm)	Tilt duration (mins)
POTS	14.1 \pm 1.9	1M, 5F	91	123	30
Syncope	11.1 \pm 3	3M, 3F	99	118	10~20
Healthy Controls	21.1 \pm 2.6	2M, 4F	72	85	30

Table 3.1: Subjects details include the health condition type, age, gender and heart rate before,during and after the tilt.

3.1.1 Healthy Controls

The 6 healthy control data were collected in the University of Wisconsin-Milwaukee. Healthy control subjects (age 18-24 years) were volunteered to this study. And they were consented and questioned before the procedure. That they could be on no medications and had no history of fainting, or lightheadedness with standing in the last year. The difference between the 6 patients who completed the protocol and 6 healthy control subjects is considered.

3.2 Epilepsy Experiment Protocol

All the Epilepsy patients were recruited at Children's Hospital of Wisconsin; n=4 subjects were monitored while undergoing a standard of care neurological exam. All these patients were recorded that they had seizures in last 24 hours. As part of this exam, they were subjected to attach the NIRS cytoxiometer probe to the forehead as shown in the fig 3.3. And in addition to the cytoxiometer, a NIRS probes from Hitachi (ETC 4000 NIRS, Hitachi, USA) were attached to the back of the head. This Hitachi probe only gives the hemoglobin changes. And this protocol is in progress of obtaining signals.



Figure 3.3 Epilepsy protocol, NIRS Cytosimeter is attached at forehead of the subject and Hitachi NIRS probes are attached at back of the head.

3.3 Clinical Data

3.3.1 POTS and Healthy controls Clinical data

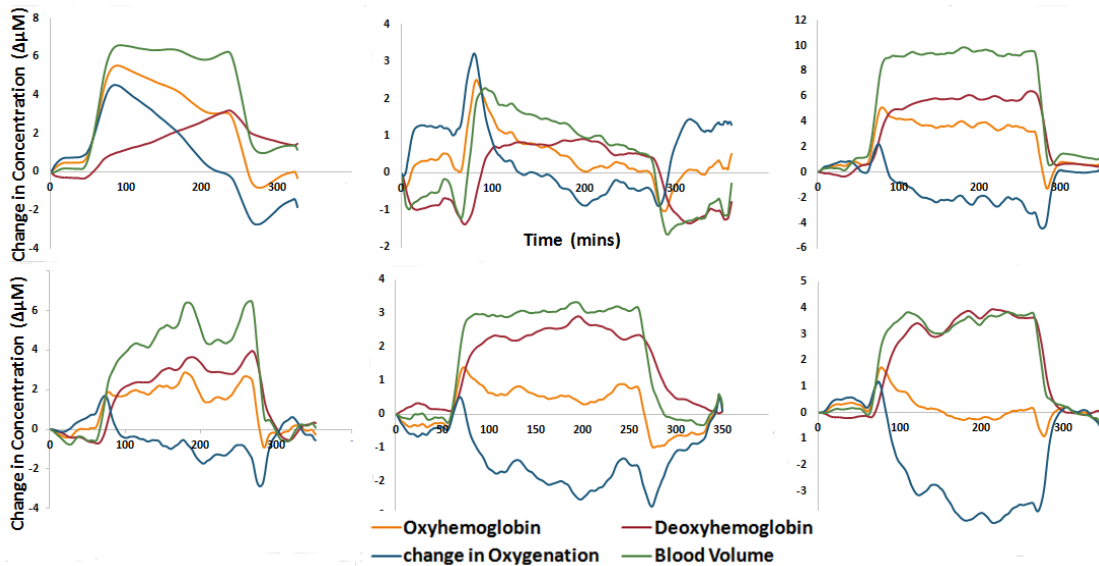


Figure 3.4 Results of Tilt table test on healthy subjects $n=6$, showing hemodynamic changes.

3.3.1.1 Validation of device

NIRS oximetry probe monitors the oxygenation change. Along with this NIRS probe, as a reference a different oximeter which is commercially available device in the market to monitor the oxygenation change (INVOS 5100B Covidien, USA). Figure 3.5 shows the correlation graph between the two probe's oxygenation change. The data is shown for both the healthy controls and POTS patients at the baseline, 70° tilt and recovery. Regional oxygenation change parameter for Covidien Oximetry device is 'percentage' (%), whereas for NIRS probe device's oxygenation change parameter is 'concentration'(microMolar or μM).

During the 70° tilt, the data trend is similar for oxygenation change in both Covidien Oximetry device and NIRS probe device for healthy subjects and POTS patients. The value of R^2 closer to 1.0 shows the better fit of the regression line between Covidien probe and custom build NIRS oximetry probe.

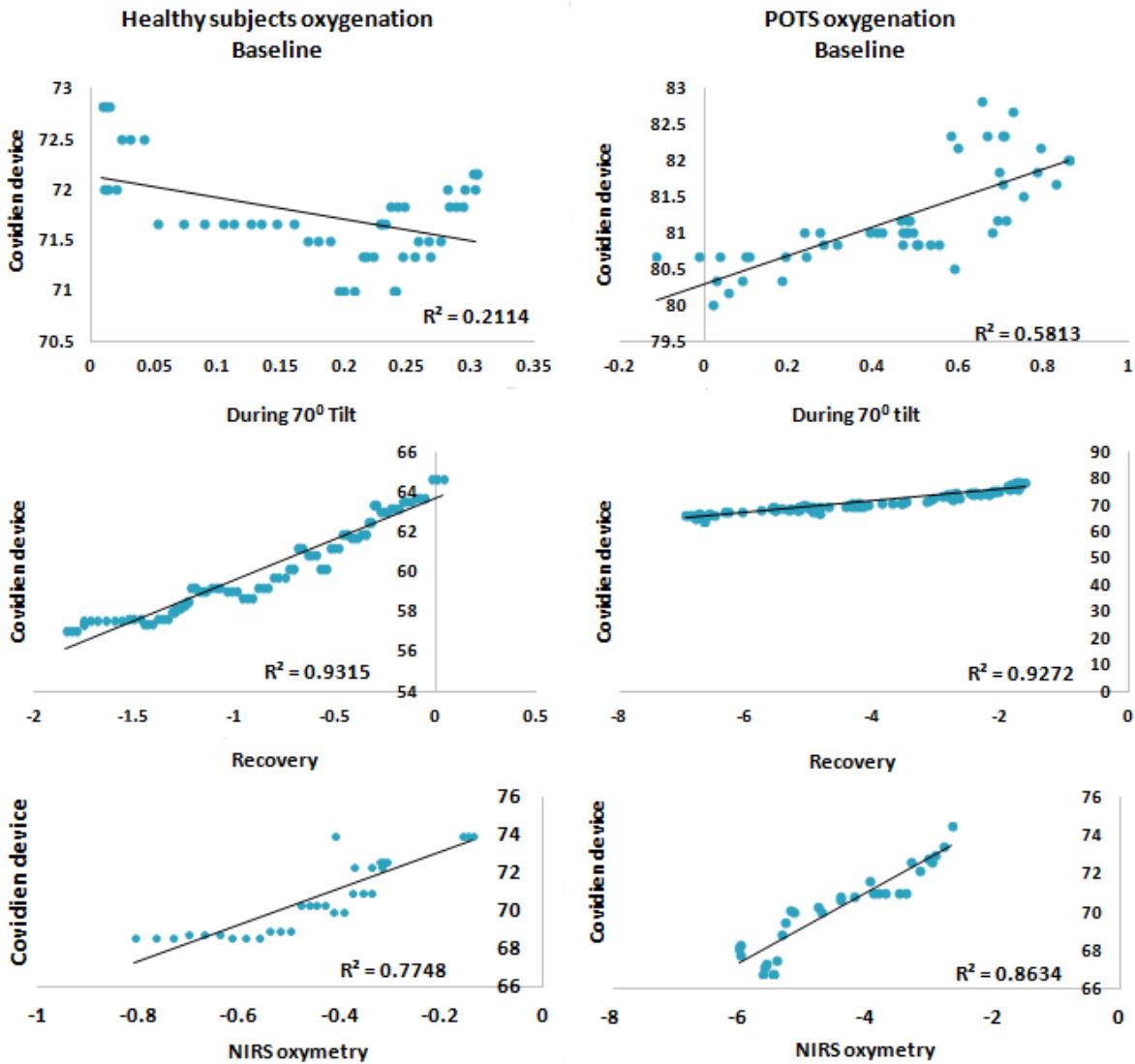


Figure 3.5 Regional Oxygenation change correlation graph between Covidien probe and NIRS oximetry Probe results in POTS and healthy controls subjects during baseline, tilt at 70° and recovery. R^2 on the graphs closer to 1.0 show the better fit of the regression line.

3.3.1.2 Physiological findings

Figure 3.6 shows average oxy-hemoglobin (ΔC_{HbO_2}) and deoxyhemoglobin (ΔC_{Hb}) data collected from the healthy control subjects and patients with POTS. The three segments show the change in the posture of the subject from 0° (baseline) to 70° (tilt) and back to 0° (recovery).

Oxy-hemoglobin decreases during the 70° tilt in healthy subjects, and Deoxy-hemoglobin increases during the same time. For POTS patients, the direction is similar, i.e. increase in deoxy-hemoglobin and decrease in Oxy-hemoglobin but the rise in deoxy-hemoglobin concentration in POTS patients is significantly greater than the rise in healthy subjects. Statistics are shown in Fig 3.6.

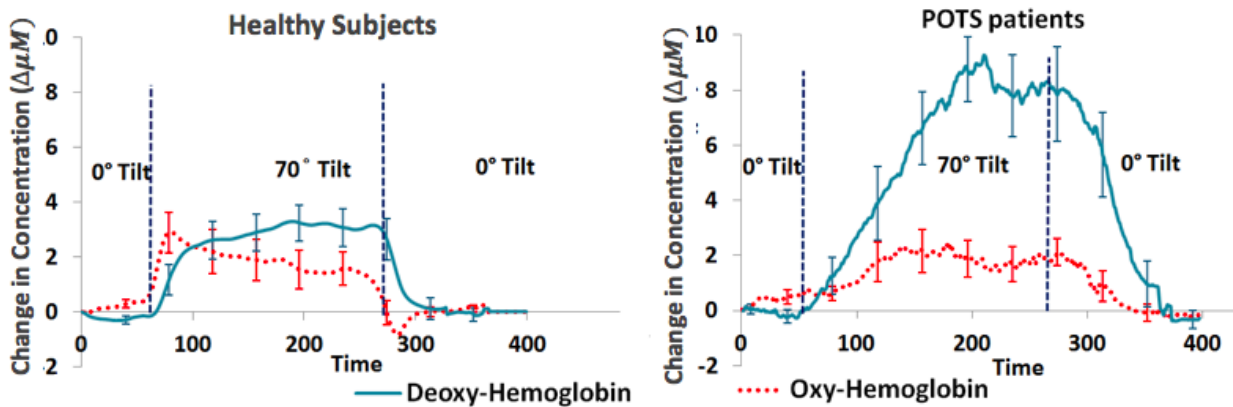


Figure 3.6 Data comparison between Healthy subjects (non-POTS) and POTS patients depicts changes in average oxy-hemoglobin (HbO₂) and deoxy-hemoglobin (Hb) concentrations on changing the position of the tilt table at 0°, 70° and 0° for 10 mins, 30 mins and 10 mins respectively.

3.3.1.3 Statistical differences

In Fig. 3.7, the statistical analysis, each bar represents the averages of the oxyhemoglobin, deoxyhemoglobin, change in oxygenation and blood volume for both groups POTS and healthy subjects during the 70° tilt.

The Student’s two-tailed t-test ($p < 0.01$) is applied to the values of the signals to test for significant differences. From the figure, the oxyhemoglobin did not show any difference, deoxyhemoglobin showed significant difference in POTS patients and healthy controls. Hb levels showed a significant difference between patient and healthy subjects which has a p-value. The

observed difference shows that deoxy-hemoglobin is significantly more in patients with POTS than in healthy controls.

Oxygenation change in patient and healthy controls has shown a significant difference with $p < 0.01$. The drop of change in oxygenation concentration in POTS patients is significantly greater than in healthy control subjects. Blood volume changes in patients with POTS is more than healthy controls.

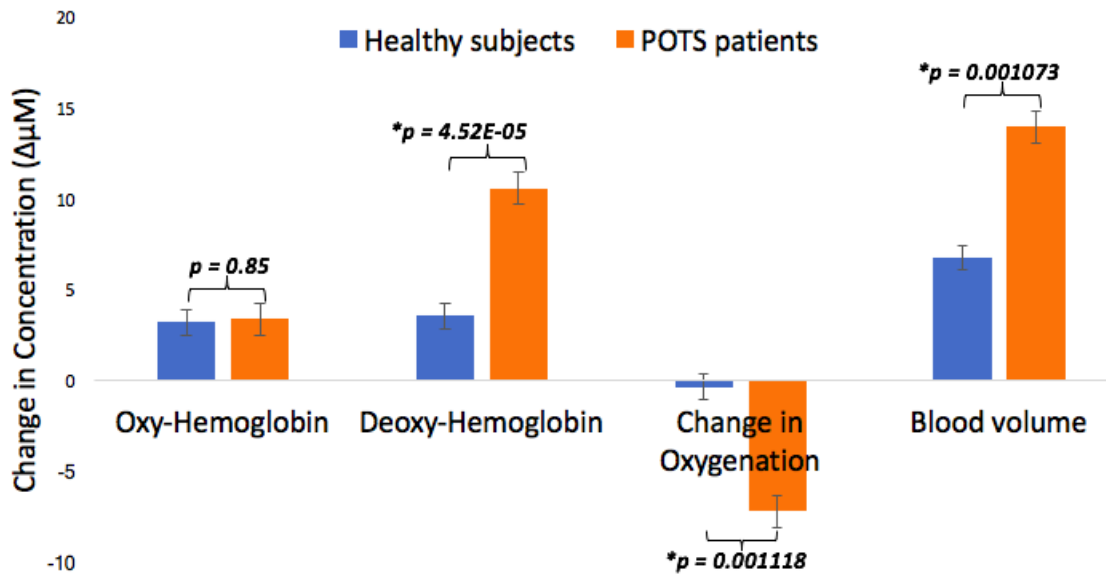


Figure 3.7 Statistical analyses for hemodynamic changes in healthy subjects and patients with POTS. Change in average oxy-hemoglobin, hemoglobin, change in oxygenation (oxygen saturation) and blood volume in control subjects during the 70° tilt. Referring p-value is < 0.01 .

3.3.2 Epilepsy Clinical data

Ambient light and baseline levels of the light were obtained after the application of the probe on the head. The results of the commercial Hitachi oximeter probes were used to verify the measurements made by the cytoxicimeter probe. Epileptic patients need constant monitoring which could be done by the cytoxicimeter device to show the blood oxygenation changes and metabolic

activity by the redox state of CCO. The process of monitoring is still in process, the results show the oxyhemoglobin and deoxyhemoglobin along with the CCO redox state. The patient had epileptic seizures in last 24 hours. The results were monitored when the patient is not having the seizures.

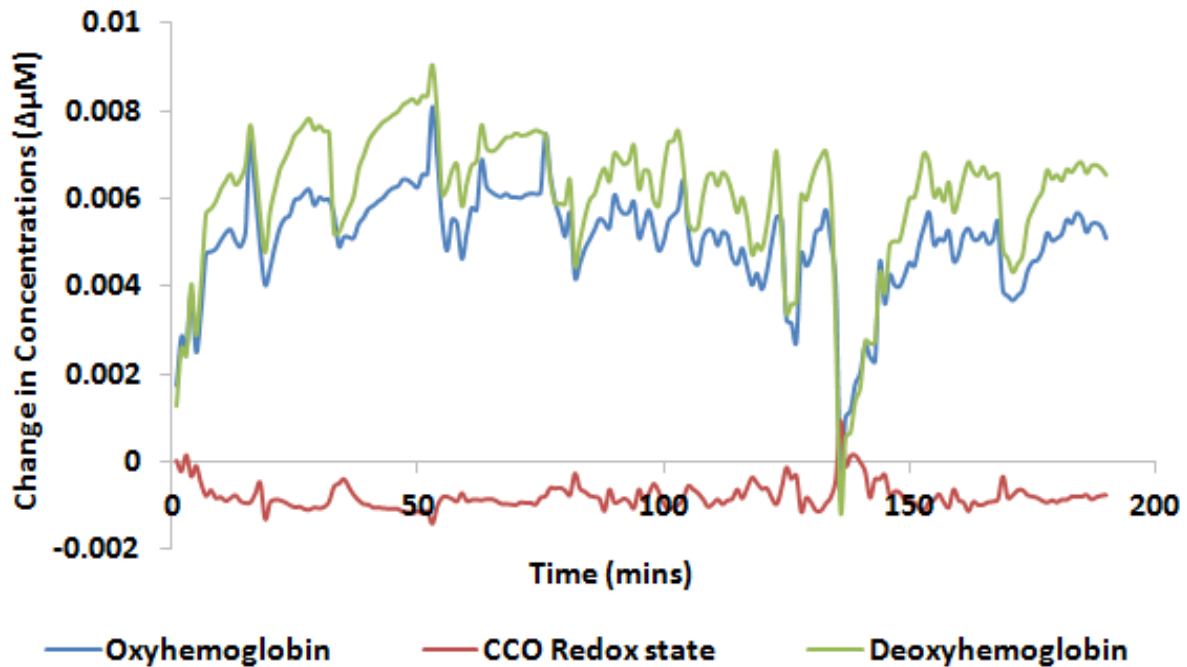


Figure 3.5 Epilepsy representative monitored raw data

3.4 Research Protocol result

This research protocol was employed in order to show the CCO redox state, oxyhemoglobin and deoxyhemoglobin changes with the muscular exercise effort.

3.4.1 Pressure Cuff Experiment

The results of pressure cuff forearm ischemia experiment are shown in Fig 3.9. A 5 minutes baseline is obtained and then rapidly pressure applied up to 240 mmHg for about 5 minutes in the cuff which is attached to the subject. The recovery is done for 5 minutes.

The results showed the same trends as in ischemia results from the publication [37], increase in deoxyhemoglobin and decrease in oxyhemoglobin where rapid pressurizing caused ischemia in the forearm muscle. That shows the ability of the probe to detect hemoglobin changes.

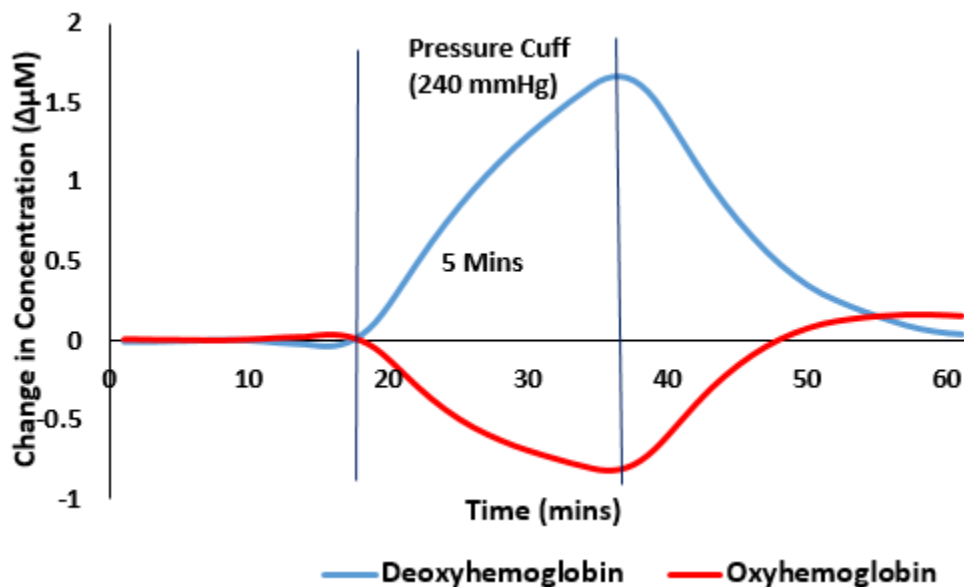


Figure 3.6 Pressure Cuff results

3.4.2 Force Plate Experiment

The probe was attached to the calf muscle of the subject. The subjects were asked to place their foot on the apparatus and raise the heel to apply the force on the strain gauge in force measuring direction. This exercise was repeated at three intervals by a change in the applied force 80%, 60% and 40% of their respective maximum which was set at starting of the protocol in LabVIEW software. The results of the cytoximeter data of one of the representative are seen in the figure.

The results show that, with an increased metabolic activity of the muscle, the CCO redox state increases at each level of exercise. The oxyhemoglobin decreases, due to increase in metabolic activity and consumption of oxygen. This gives an increase in deoxyhemoglobin. During the rest, the metabolic activity decreases so the trends of oxyhemoglobin, deoxyhemoglobin and CCO redox state were opposite to the exercise results.

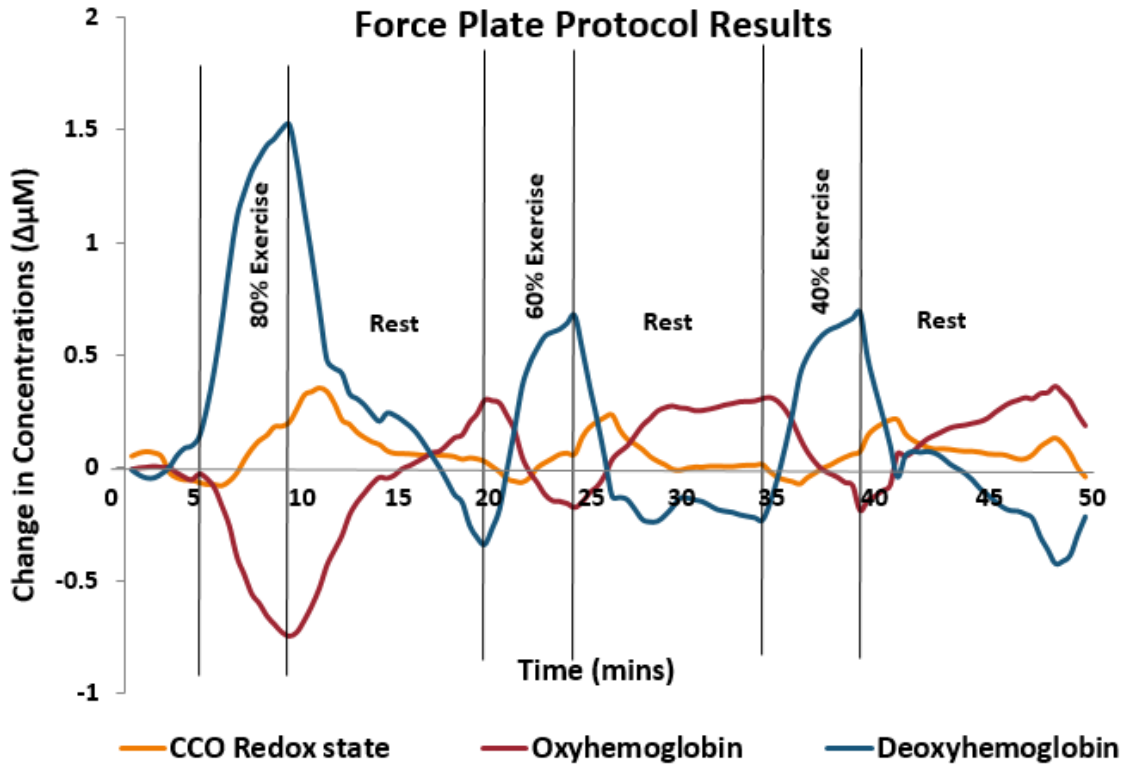


Figure 3.7 The results from a force plate experiment. As the subject apply force measured by strain gauge at 80%, 60% and 40% exercise levels.

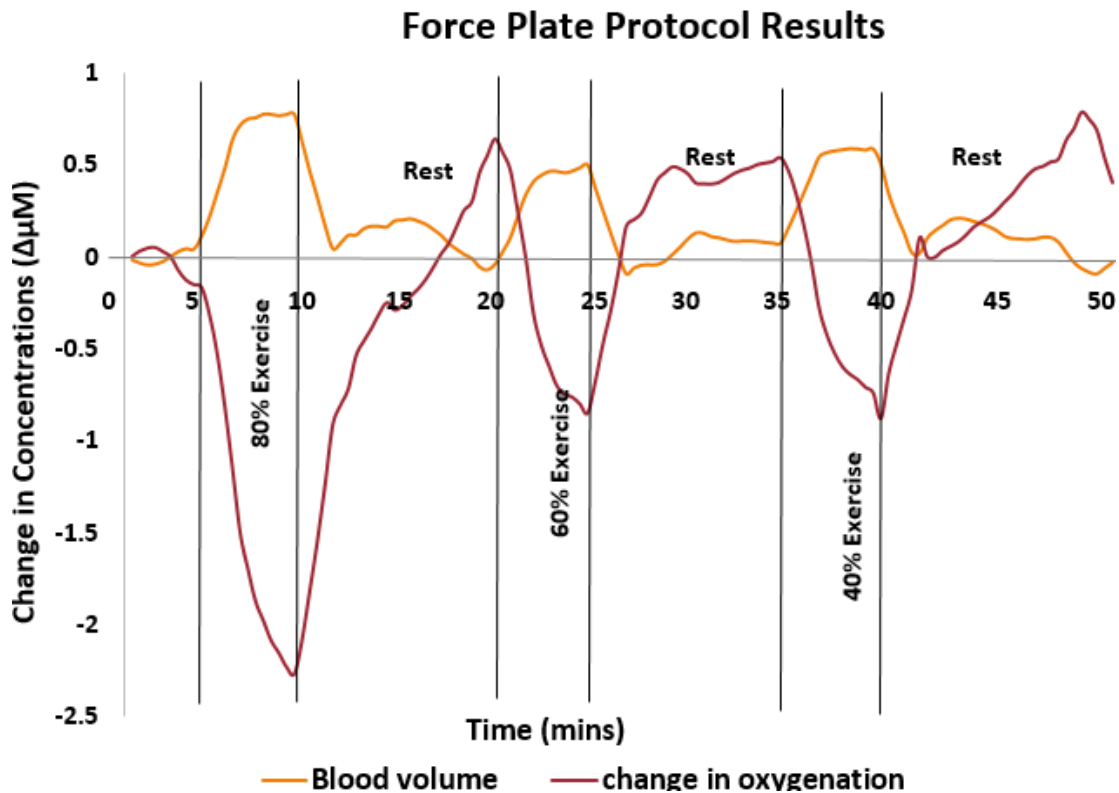


Figure 3.8 The blood volume and change in oxygenation results of the force plate at different exercise levels.

Figure 3.11: The decrease of oxygenation and increase in blood volume is shown during the exercise according to the range of metabolic activity. Thus, from the results, we see what we expect to see with range of metabolic activity on the 80%, 60% and 40% of maximum exercises.

Conclusion and Discussion

The goal of these experiments was to detect the change in hemoglobin along with the changes in CCO signal. These results have shown the custom-built device can measure the redox state of CCO along with changes in hemoglobin. Such device will assess the health of the patients that need constant monitoring of the metabolic actives and change in oxygenation of the tissue.

The tilt table tests demonstrated that the subjects are experiencing venous pooling during the tilt. The hemodynamic changes observed during the tilt suggests that subjects have experience

the venous pooling by effective change in their legs blood volume. The remarkable differences in the pattern of change in HbO₂ and Hb may provide a new understanding of the underlying pathophysiology of POTS. Healthy subjects show a sharp rise in HbO₂ that is quickly halted within the first 2 minutes upright, while POTS patients take about 10 minutes to rise to the same level. Thus, the slope of rising of HbO₂ differs markedly between the 2 groups.

The force plate exercise has demonstrated that exercise levels effect on the amount of metabolic actives by redox state of CCO. And the Pressure cuff experiment showed the device could monitor the hemoglobin changes.

4. Conclusion and Future Work

4.1 Conclusion

I have designed the second version of Cytoximeter which has Laser diodes as the source. This Cytoximeter could successfully monitor the hemoglobin signal along with CCO signal. Applied the cytoximeter to muscle in different protocols and acquired objective means of results according to the metabolic activity.

Coming to the clinical setting, the cytoximeter was applied to POTS patient and healthy controls to obtain the significant difference between POTS affected subjects and controls, as well as produce new physiological findings. This study investigates the potential use of NIRS spectroscopy for the quantitative measurement of calf hemodynamics in POTS patients and healthy controls. The custom-built probe was applied to study the hemodynamics in the calf muscle of patients suffering from POTS during a change in posture with heads up tilt table. This could potentially help in determining whether tissue tonicity plays a role in the symptoms experienced by POTS patients. Such results could be used to quantitatively track the progress of a therapy in terms of changes in muscle oxygenation. Another application would be in POTS examinations, as a means of providing objective evidence of the degree of the syndrome. The cytoximeter can be used as a clinical tool to acquire muscle or brain oximetry data from patients suffering from POTS and Epileptic seizures. The results of that study showed the ability of NIRS and its applications in the clinical settings.

4.2 Future Work

In clinical near-infrared spectroscopy (NIRS), movements of the subject often cannot be controlled. That can cause significant step changes in the baselines measurements of attenuated

signals [7].

The manual identification and correcting this motion artifact in NIRS data is time-consuming and may even be useless because it may lose valuable data. Updating the NIRS device by an automated method for identifying and correcting motion artifacts. An accelerometer-based motion artifact can provide long term application of NIRS.

Bibliography

- [1] F. F. Jobsis, "Noninvasive, infrared monitoring of cerebral and myocardial oxygen sufficiency and circulatory parameters," *Science*, vol. 198, no. 4323, pp. 1264-1267, 1977.
- [2] F. F. Jobsis-vander Vliet, "Discovery of the near-infrared window into the body and the early development of near-infrared spectroscopy," *Journal of biomedical optics*, vol. 4, no. 4, pp. 392-397, 1999.
- [3] M.-C. Taillefer and A. Y. Denault, "Cerebral near-infrared spectroscopy in adult heart surgery: systematic review of its clinical efficacy," *Canadian Journal of Anesthesia*, vol. 52, no. 1, p. 79, 2005.
- [4] H. Tanaka, R. Matsushima, H. Tamai, and Y. Kajimoto, "Impaired postural cerebral hemodynamics in young patients with chronic fatigue with and without orthostatic intolerance," *The Journal of Pediatrics*, vol. 140, no. 4, pp. 412-417, 2002/04/01/ 2002.
- [5] R. Boushel, H. Langberg, J. Olesen, J. Gonzales-Alonzo, J. Bülow, and M. Kjaer, "Monitoring tissue oxygen availability with near infrared spectroscopy (NIRS) in health and disease," *Scandinavian journal of medicine & science in sports*, vol. 11, no. 4, pp. 213-222, 2001.
- [6] G. Bale, C. E. Elwell, and I. Tachtsidis, "From Jöbsis to the present day: a review of clinical near-infrared spectroscopy measurements of cerebral cytochrome-c-oxidase," *Journal of biomedical optics*, vol. 21, no. 9, pp. 091307-091307, 2016.
- [7] J. Virtanen, T. Noponen, K. Kotilahti, J. Virtanen, and R. J. Ilmoniemi, "Accelerometer-based method for correcting signal baseline changes caused by motion artifacts in medical near-infrared spectroscopy," *Journal of biomedical optics*, vol. 16, no. 8, pp. 087005-087005-9, 2011.
- [8] J. E. Jones, J. K. Austin, R. Caplan, D. Dunn, S. Plioplys, and J. A. Salpekar, "Psychiatric disorders in children and adolescents who have epilepsy," *Pediatrics in Review*, vol. 29, no. 2, 2008.
- [9] A. Yodh and B. Chance, "Spectroscopy and imaging with diffusing light," *Physics Today*, vol. 48, no. 3, pp. 34-41, 1995.
- [10] V. Kuz'mich and V. Zharov, "Basic principles and characteristics of transcutaneous" reflective" oximetry," *Meditsinskaia tekhnika*, no. 3, pp. 36-42, 1993.
- [11] W. W. Linz, "Surface near-infrared spectroscopy and its application to stroke patients," The University of Wisconsin-Milwaukee, 2014.
- [12] R. V. Maikala, "Modified Beer's Law—historical perspectives and relevance in near-infrared monitoring of optical properties of human tissue," *International Journal of Industrial Ergonomics*, vol. 40, no. 2, pp. 125-134, 2010.
- [13] J. Sugar, "Monitoring cellular metabolism with near-infrared spectroscopy," The University of Wisconsin-Milwaukee, 2016.
- [14] K. N. Wu, E. Lieber, P. Siddarth, K. Smith, R. Sankar, and R. Caplan, "Dealing with epilepsy: parents speak up," *Epilepsy & Behavior*, vol. 13, no. 1, pp. 131-138, 2008.
- [15] C. Cooper *et al.*, "Near-infrared spectroscopy of the brain: relevance to cytochrome oxidase bioenergetics," ed: Portland Press Limited, 1994.
- [16] Y. Lin, G. Lech, S. Nioka, X. Intes, and B. Chance, "Noninvasive, low-noise, fast imaging of blood volume and deoxygenation changes in muscles using light-emitting diode continuous-wave imager," *Review of Scientific Instruments*, vol. 73, no. 8, pp. 3065-3074, 2002.
- [17] M. BRUNORI, G. ANTONINI, F. MALATESTA, P. SARTI, and M. T. WILSON, "Cytochrome-c oxidase," *The FEBS Journal*, vol. 169, no. 1, pp. 1-8, 1987.
- [18] H. Michel, J. Behr, A. Harrenga, and A. Kannt, "Cytochrome c oxidase: structure and spectroscopy," *Annual review of biophysics and biomolecular structure*, vol. 27, no. 1, pp. 329-356, 1998.

- [19] W. H. Vanneste, "The stoichiometry and absorption spectra of components a and a₃ in cytochrome c oxidase," *Biochemistry*, vol. 5, no. 3, pp. 838-848, 1966.
- [20] M. MasoudiMotlagh *et al.*, "Monitoring hemodynamic changes in stroke-affected muscles using near-infrared spectroscopy," *Journal of Rehabilitation and Assistive Technologies Engineering*, vol. 2, p. 2055668315614195, 2015.
- [21] D. A. Boas, J. Culver, J. Stott, and A. Dunn, "Three dimensional Monte Carlo code for photon migration through complex heterogeneous media including the adult human head," *Optics express*, vol. 10, no. 3, pp. 159-170, 2002.
- [22] L. Wang, S. L. Jacques, and L. Zheng, "MCML—Monte Carlo modeling of light transport in multi-layered tissues," *Computer methods and programs in biomedicine*, vol. 47, no. 2, pp. 131-146, 1995.
- [23] M. Ferrari, T. Binzoni, and V. Quaresima, "Oxidative metabolism in muscle," *Philosophical Transactions of the Royal Society of London B: Biological Sciences*, vol. 352, no. 1354, pp. 677-683, 1997.
- [24] E. G. Trapp, D. J. Chisholm, and S. H. Boutcher, "Metabolic response of trained and untrained women during high-intensity intermittent cycle exercise," *American Journal of Physiology-Regulatory, Integrative and Comparative Physiology*, vol. 293, no. 6, pp. R2370-R2375, 2007.
- [25] D. J. Faber, M. C. Aalders, E. G. Mik, B. A. Hooper, M. J. van Gemert, and T. G. van Leeuwen, "Oxygen saturation-dependent absorption and scattering of blood," *Physical review letters*, vol. 93, no. 2, p. 028102, 2004.
- [26] J. M. Stewart, M. S. Medow, and L. D. Montgomery, "Local vascular responses affecting blood flow in postural tachycardia syndrome," *American Journal of Physiology-Heart and Circulatory Physiology*, vol. 285, no. 6, pp. H2749-H2756, 2003.
- [27] C. C. Murphy, E. Trevathan, and M. Yeargin-Allsopp, "Prevalence of epilepsy and epileptic seizures in 10-year-old children: Results from the metropolitan Atlanta developmental disabilities study," *Epilepsia*, vol. 36, no. 9, pp. 866-872, 1995.
- [28] G. A. Baker *et al.*, "Perceived impact of epilepsy in teenagers and young adults: an international survey," *Epilepsy & Behavior*, vol. 12, no. 3, pp. 395-401, 2008.
- [29] M. Raspall-Chaure, B. G. Neville, and R. C. Scott, "The medical management of the epilepsies in children: conceptual and practical considerations," *The Lancet Neurology*, vol. 7, no. 1, pp. 57-69, 2008.
- [30] P. Monrad *et al.*, "Haemodynamic response associated with both ictal and interictal epileptiform activity using simultaneous video electroencephalography/near infrared spectroscopy in a within-subject study," *Journal of near infrared spectroscopy*, vol. 23, no. 4, pp. 209-218, 2015.
- [31] T. Nguyen, S. Ahn, H. Jang, S. C. Jun, and J. G. Kim, "Utilization of a combined EEG/NIRS system to predict driver drowsiness," *Scientific Reports*, vol. 7, 2017.
- [32] F. van Bel, C. A. Dorrepaal, M. J. Benders, P. E. Zeeuwe, M. van de Bor, and H. M. Bergen, "Changes in cerebral hemodynamics and oxygenation in the first 24 hours after birth asphyxia," *Pediatrics*, vol. 92, no. 3, pp. 365-372, 1993.
- [33] J. Wyatt, "Near-infrared spectroscopy in asphyxial brain injury," *Clinics in perinatology*, vol. 20, no. 2, pp. 369-378, 1993.
- [34] R. Cubeddu, A. Pifferi, P. Taroni, A. Torricelli, and G. Valentini, "A solid tissue phantom for photon migration studies," *Physics in medicine and biology*, vol. 42, no. 10, p. 1971, 1997.
- [35] P. Di Ninni, F. Martelli, and G. Zaccanti, "Effect of dependent scattering on the optical properties of Intralipid tissue phantoms," *Biomedical optics express*, vol. 2, no. 8, pp. 2265-2278, 2011.
- [36] S. J. Madsen, M. S. Patterson, and B. C. Wilson, "The use of India ink as an optical absorber in tissue-simulating phantoms," *Physics in medicine and biology*, vol. 37, no. 4, p. 985, 1992.

- [37] S. Matcher, C. Elwell, C. Cooper, M. Cope, and D. Delpy, "Performance comparison of several published tissue near-infrared spectroscopy algorithms," *Analytical biochemistry*, vol. 227, no. 1, pp. 54-68, 1995.